

2 Quantifying late-Holocene climate in the Ecuadorian Andes using a chironomid-based temperature
3 inference model

4 Frazer Matthews-Bird; Stephen J. Brooks; Philip B. Holden; Encarni Montoya, and William D. Gosling

5 We wish to thank all the reviewers involved in the preparation of this manuscript, and the editorial
6 board of *Climate of the Past* for the opportunity to submit a revised version of the original manuscript. We
7 feel the extended review process has resulted in a superior study, which will appeal to a broad readership
8 and make a significant contribution to the field. Below is a detailed breakdown of how the latest round of
9 reviewer comments have been addressed.

10 Referee #1: *I would like to commend the authors for thoroughly engaging with the reviewers' comments and*
11 *making substantive changes to the ms. I believe the ms greatly improved and deserving of publication. I look*
12 *forward to seeing the ms published.*

13 Anonymous Referee #2: comment 1

14 *The authors have addressed the issues adequately. The changes are well documented. However, in accordance*
15 *with the revised text body, also the Abstract must be modified (mention the caveats of the TF and the*
16 *reconstruction in L Pindo) in the sense that the reconstruction is qualitative; (e.g. add 1-2 sentences Line 487*
17 *- 489 and/or Lines 687-689).*

18
19 **Response to Referee #2: comment 1**

20 We have modified the abstract in line with the reviewer's comments. Lines 20-23 now reads:

21 *We would caution, however, against an over interpretation at this stage. The reconstruction can only*
22 *currently be deemed qualitative and requires more research before quantitative estimates can be generated*
23 *with confidence.*

24
25 Anonymous Referee #2: comment 2

26 *Maybe I have missed it in the text, but it should be mentioned somewhere that all data (Transfer*
27 *Function and Downcore stratigraphy) are publicly available at www.xy (NERC website). This is very*
28 *important.*

29
30 **Response to Referee #2: comment 2**

31 The data is stored with the National Geoscience Data Centre (NGDC) and can be found at
32 <http://www.bgs.ac.uk/downloads/home.html>. The data repository process can take 3 months to finalize
33 before a DOI is issued, however we understand the data can be accessed using the repository search
34 engine. This link has now been included in the acknowledgments, however, we would also be happy to
35 make the data available as supplementary information. We leave that decision to the editorial board.

36
37 Anonymous Referee #2: comment 3

38 *It's a question of style, but Sections 4.1 and 4.3 are very short (just two sentences or so). Maybe combine L411:*
39 *929 cm.*

40
41 **Response to Referee #2: comment 2**

42 Section 4: Results now has just three subsections in line with reviewer's comments.

43 4. Results

44 4.1 Calibration data set

45 4.2 Laguna Pindo fossil chironomids and dating.

46 4.3 Palaeotemperature reconstructions

47 **Inferring late-Holocene climate in the Ecuadorian Andes using a chironomid-based temperature inference**

48 **model**

49

50 Frazer Matthews-Bird^{1&2}, matthewsbirdf@fit.edu

51 Stephen J. Brooks³, S.Brooks@nhm.ac.uk

52 Philip B. Holden¹, philip.holden@open.ac.uk

53 Encarni Montoya¹, encarni.montoya@open.ac.uk

54 William D. Gosling^{1,4}, W.D.Gosling@uva.nl

55 ¹Department of Earth, Environment & Ecosystems, The Open University, Walton Hall, Milton Keynes, MK7 6AA,
56 UK.

57 ²Biological Sciences, Florida Institute of Technology, 150 West University Boulevard, Melbourne, FL 32901, USA

58 ³Department of Life Sciences, Natural History Museum, Cromwell Road, London SW7 5BD, UK.

59 ⁴Palaeoecology & Landscape Ecology, Institute for Biodiversity & Ecosystem Dynamics, University of
60 Amsterdam, P.O. Box 94248, 1090 GE Amsterdam, The Netherlands

61 **Corresponding author:** Frazer Matthews-Bird

62

63 **Key words:** Bayesian, weighted-averaging, transfer function, chironomids, Holocene climate change, Ecuador

64

65

66

67

68

69

frazer 2/26/2016 3:21 PM

Deleted: Quantifying

71 **1. Introduction**

72 Holocene climate variability (11.7 kcal yrs BP – present) offers the most recent opportunity to
73 parameterise climate and ecosystem responses to natural forcing under current boundary conditions in the
74 absence of intense anthropogenic activity (Mayewski *et al.*, 2004; Oldfield and Steffen, 2014). Furthermore,
75 quantitative estimates of past climate over long time scales (>1000 yrs) are vital to improving the reliability of
76 modelling and prediction of present and future climate variability (Mayewski *et al.*, 2004). The spatial
77 distribution of palaeoclimate records, however, is currently uneven around the world. Quantitative
78 reconstructions of past climate are common from mid- to high- latitudes of both hemispheres but data is much
79 scarcer from low-latitude (tropical) regions (Jansen *et al.*, 2007). Tropical climate is the dominant driver of
80 atmospheric circulation (Ivanochko *et al.*, 2005) and the source of intermittent phenomena, such as the El Niño
81 Southern Oscillation (ENSO), which has a global influence on climate (Collins *et al.*, 2010). Quantitative
82 estimates of past climate from the low latitude tropics, therefore, are crucial for investigating not only regional
83 climate processes, but also teleconnections on long timescales (>1000 years) (Garreaud *et al.*, 2009; Jomelli *et*
84 *al.*, 2009; Vuille *et al.*, 2000). Here we develop the first chironomid-based temperature inference model for
85 tropical South America. The model is applied to a Holocene lake sediment sequence to generate a chironomid-
86 inferred temperature reconstruction from the tropical East Andean flank.

87 Chironomidae (non-biting midges) is a family of two-winged aquatic insects of the order Diptera. The
88 family is globally distributed and one of the most diverse within aquatic ecosystems (Armitage *et al.*, 1995).
89 Many species are stenotopic, and their short life-cycles and ability to colonise favourable regions quickly means
90 the insects are extremely sensitive to environmental change (Pinder, 1986). The head capsules of chironomid
91 larvae are well preserved in lake sediments and have been used extensively as palaeoecological proxies (Brooks,
92 2006; Walker and Cwynar, 2006). Chironomid-based temperature inference models, derived from modern
93 calibration data sets, have been applied across North America (reviewed in Walker and Cwynar, 2006), Eurasia
94 (reviewed in Brooks, 2006), and more recently the method has been applied in the Southern Hemisphere in
95 Patagonia (Massferro and Larocque, 2013; Massferro *et al.*, 2014), Central America (Wu *et al.*, 2014), East
96 Africa (Eggermont *et al.*, 2010), and Australasia (Dimitriadis and Cranston 2001; Woodward and Shulmeister
97 2006).

frazer 2/25/2016 10:27 AM
Deleted: the first quantitative
frazer 2/25/2016 10:27 AM
Deleted: s

frazer 2/25/2016 1:38 PM
Deleted: r

101 Transfer functions make a number of underlying assumptions; particularly the environmental variable to be
102 reconstructed is an ecologically important determinant in the system, and environmental variables other than
103 one being reconstructed have a negligible effect on species assemblages (Juggins, 2013). Rarely are ecological
104 systems as simple as transfer functions would imply and violations of these assumptions will undermine the
105 validity of the environmental reconstruction (Juggins, 2013). Nevertheless, despite known inherent problems
106 associated with transfer functions (Huntley, 2012; Juggins, 2013; Velle *et al.*, 2010), quantitative reconstructions
107 from chironomid assemblages often produce consistent results that compare well with other proxy estimates of
108 past temperature (Brooks, 2000; Brooks *et al.*, 2012; Heiri *et al.*, 2007). The best performing inference models
109 can reconstruct temperatures with errors of c. 1°C (Brooks and Birks, 2001; Eggermont *et al.*, 2010; Heiri *et al.*,
110 2003; Olander *et al.*, 1999a; Rees *et al.*, 2008; Self *et al.*, 2011) providing high resolution insights into past
111 changes in climate (Brooks and Langdon, 2014), and validation of climate models (Heiri *et al.*, 2014).

112

113 1.1 Holocene climate variability

114 Holocene climate variability is subdued ($\pm 2-3^{\circ}\text{C}$) (Mayewski *et al.*, 2004; O'Brien *et al.*, 1995) compared with
115 the preceding Late Glacial (c. 15,000-11,700 years before present [yrs BP], $\pm 7-10^{\circ}\text{C}$) (Alley, 2000; Anderson,
116 1997), nevertheless rapid climate change events are recognised in Holocene palaeoclimate records (Marcott *et al.*,
117 2013; Mayewski *et al.*, 2004). Changes in insolation caused by solar forcing, generally regarded as the
118 dominant driver of global climate change during the Holocene (Mayewski *et al.*, 2004; Wanner *et al.*, 2008). The
119 Roman warm period (250 BC-400 AD [2200-1550 yrs BP]), and cooling during the Little Ice Age (LIA) (1350-1850
120 AD [600-100 yrs BP]) are well established features, notably across the Northern Hemisphere (Johnsen *et al.*,
121 2001; O'Brien *et al.*, 1995). Some evidence from the tropics suggests Holocene climate fluctuations such as the
122 LIA maybe global events (Thompson *et al.*, 2002; Wanner *et al.*, 2008); however, additional quantitative
123 palaeoclimate records are needed to understand the expression of such events in the tropics, and to clarify
124 global climate teleconnections. Although the low latitudes receive 47% of planetary insolation, the climate
125 response in the tropics to solar variability is poorly understood (Crowley, 2000; Polissar *et al.*, 2006).

126

127

frazer 2/25/2016 1:41 PM

Deleted: period

frazer 2/25/2016 1:41 PM

Deleted: 25

frazer 2/25/2016 3:44 PM

Deleted: is

frazer 2/25/2016 1:47 PM

Deleted: Growing

frazer 2/25/2016 1:48 PM

Deleted: are probably

133 **1.2 Holocene climate variability in tropical South America**

134 The most notable feature of current South American climate is the annual migration of the Intertropical
135 Convergence Zone (ITCZ), which affects rainfall patterns across the tropical Andes (Garreaud et al., 2009;
136 Hastenrath, 2012). On Holocene timescales, however, there remain large uncertainties regarding the patterns
137 and processes of climate change in the Andes with evidence for both rapid (c. 100-1000 yr) precipitation (Haug
138 et al., 2001) and temperature (Thompson et al., 2006; Wanner et al., 2008). A further point to note is the spatial
139 heterogeneity of Holocene climate variability in the tropical Andes (Baker and Fritz, 2015a), particularly
140 regarding precipitation. Ice core records from the Peruvian and Bolivian Andes since c. 5400 cal yrs BP suggest
141 the overall trend is towards a drier climate with high amplitude fluctuations and periods of significant aridity.
142 Precipitation reached a minimum during the period between 3800-2800 cal yrs BP and the LIA (Haug et al.,
143 2001; Thompson et al., 1986; Thompson et al., 1995). Speleothem records from the Central Andes of Peru
144 contradict this, however, and indicate instead that from the 15th to 18th century precipitation was on average
145 about 10% higher than the present day (Reuter et al., 2009).

146 The mid- to late-Holocene (c. 6000 cal yrs BP to present) is a period of cooling climate in South America.
147 Pollen evidence suggests montane vegetation replaced Andean forest taxa as the treeline lowered with modern
148 vegetation patterns becoming established by c. 3000 cal yrs BP (Markgraf, 1989). Long-term cooling in the late
149 Holocene culminated in a minimum during the 17th and 18th centuries, coinciding with evidence for precipitation
150 minimum during the LIA in northern South America (Haug et al., 2001; Thompson et al., 1986; Thompson et al.,
151 1995). Further south, Patagonian proxy records infer periods that were wet and cold enough to allow glacial
152 advance (Meyer and Wagner, 2008). In the South American tropics, where the relationship between changes in
153 temperature and precipitation are complex (Baker et al., 2001; Garreaud et al., 2009), more independent
154 quantitative estimates of past temperature are needed in order to resolve climate patterns over the tropical
155 Andes during the Holocene.

156
157 **1.3 Aims**

158 In this study, we have developed the first chironomid-based temperature calibration data set from the
159 tropical Andes (0 to 17°S). Surface sediment samples from 59 lakes along the eastern flank of the Andes to

frazer 2/25/2016 3:44 PM
Deleted: variability

frazer 2/26/2016 2:32 PM
Deleted: - ... [1]

163 Amazonia are analysed. Two approaches are used to develop the inference model, the widely used weighted
164 averaging method (Brooks and Birks, 2000) and a Bayesian approach (Holden *et al.*, 2008) which has rarely been
165 used before. The models are applied to fossil chironomid assemblages in a late-Holocene lake sediment record
166 from Laguna Pindo, central Ecuador, to reconstruct mean annual temperature (MAT) changes over the past c.
167 3000 years.

frazer 2/25/2016 3:45 PM

Deleted: a second using

168

169 2 Study Sites

170 2.1 Modern calibration dataset

171 Surface sediments were collected from 59 lakes across Bolivia (15 lakes), Peru (32 lakes) and Ecuador (12
172 lakes) between 2004 and 2013 over an altitudinal gradient from 150 m above sea level (a.s.l) to 4655 m a.s.l,
173 between 0-17°S and 64-78°W (Fig 1). The study sites cover an MAT of 25°C; the coldest lake in the data set is
174 0.8°C MAT and the warmest is 25°C MAT (Table 1). The deepest lake is 25 m and the shallowest is 0.1 m, mean
175 water depth of all the study sites is 5 m. Cold, high elevation lakes are more common within the calibration data
176 set and there are no lakes between 16°C and 20°C. Sediment samples used in this study were taken from the
177 uppermost centimetre (0-1cm) which represents the most recent deposits (approx. 5-20 years) (Frey, 1988) and
178 therefore most comparable with the available climate data for calibration.

frazer 2/25/2016 3:45 PM

Deleted: gradient

frazer 2/26/2016 3:46 PM

Deleted: 1

179

180 2.2 Fossil chironomid record

181 Laguna Pindo is a small shallow lake on the eastern flank of the Ecuadorian Andes (1°27.132'S;
182 78°04.847'W) (Fig1). The site is located at an elevation of 1248 m a.s.l. MAT is c. 20°C with little seasonal
183 variation and mean annual precipitation (MAP) can reach c. 4000 mm per year (Hijmans *et al.*, 2005). Currently
184 the lake is not directly fed by a stream in-flow and has no visible stream out-flow; the lake receives water from
185 surface run-off and direct precipitation. There are no obvious geomorphological causes for the escarpment of
186 the lake and we hypothesise it is tectonic in origin.

frazer 2/26/2016 2:37 PM

Deleted: -

... [2]

187 At the time of field work (January 2013) maximum water depth was c. 1 m, the lake is heavily overgrown
188 with aquatic macrophytes making a detailed bathometric survey difficult. A sedimentary sequence 929 cm long

194 was extracted using a cam-modified piston Livingston corer (Colinvaux *et al.*, 1999) from the centre of the lake
195 to minimise the chance of encountering a sedimentary gap caused by any periods of lake area reductions.
196 Sediments were recovered in aluminium tubes and sealed on site before being transported to the UK and
197 stored at c. 4°C. A total of 6 samples were analysed for ¹⁴C radiocarbon using AMS dating at the SUERC
198 radiocarbon facility, East Kilbride (Table 2). An age-depth model was created using version 2.2 of the statistical
199 package clam.R (Blaauw, 2010) and the Southern Hemisphere calibration curve SHCal13.14C (Hogg *et al.*, 2013)
200 (Fig 2). The sampling interval for chironomid analysis was not uniform due to a varied sedimentation rate. To
201 achieve as even a coverage possible over the time interval, samples were taken between every 10 and 20cm.

frazer 2/26/2016 3:37 PM

Deleted: 14

203 3. Methods

204 3.1 Chironomid analysis

205 Chironomid preparation and identification from both lake surface and core sediments followed standard
206 methods as described by Brooks *et al* (2007). The wet sediment was deflocculated in 10% KOH for 2 minutes at
207 75°C. The sediment was then washed through 212µm and 90µm sieves with water. Chironomids were picked
208 from the residues in a Bogorov counting tray using a stereomicroscope at 25x magnification. Head capsules
209 were mounted in Euparal, ventral side up and identified to the highest possible taxonomic resolution under a
210 compound light microscope at 200-400x magnifications with reference to Wiederholm (1983), Epler (2001)
211 Rieradevall & Brooks (2001), Brooks *et al* (2007), Cranston (2010) and local taxonomic works including Prat *et al*
212 (2011), and Trivinho-Strixino (2011). Some taxa could not be formally identified and so were given informal
213 names. Images and descriptions of informally named taxa are provided in Matthews-Bird *et al* (2015).

frazer 2/26/2016 3:57 PM

Formatted: Tabs: 3.61", Centered

215 3.2 Environmental variables

216 Environmental variables (depth, pH, conductivity, and water temperature) were measured at each lake in
217 the field. Organic content of the sediment was established through Loss-on-ignition following standard methods
218 as described by Heiri *et al* (2001). Climate data (MAT, MAP) were obtained from high resolution, interpolated
219 climate surfaces (Hijmans *et al.*, 2005). A summary of all the environmental variables measured can be found in
220 Table 1.

frazer 2/26/2016 2:39 PM

Deleted: Elevation (m a.s.l.), latitude (decimal degrees), and longitude (decimal degrees) were also included as variables in the calibration data set.

225
226
227
228
229
230
231
232
233
234
235
236
237
238
239
240
241
242
243
244
245
246
247
248
249
250
251

3.3 Exploratory statistics

Detrended Correspondence Analysis (DCA) was initially used as an indirect ordination method to assess the gradient lengths in compositional units of taxon turnover (Hill and Gauch, 1980). The gradient length of DCA axis 1 was 5.2 standard deviation units (SD), which suggests a unimodal response, and that linear ordination methods were not appropriate (ter Braak, 1987). Canonical Correspondence Analysis (CCA) was used to explore the influence of the measured environmental variables on the distribution and abundance of taxa. Highly correlated variables were partialled-out by analysis of the variance of their regression coefficients indicated by their Variance Inflation Factors (VIFs). Variables with high VIFs were systematically removed from the environmental variable data set until the remaining variables had VIFs below 20. Detrended canonical correspondence analysis (DCCA) was used to test how much of the variance in the assemblage data was explained by each individual explanatory variable. The ratio of $\lambda_1:\lambda_2$ (i.e., the ratio of first constrained DCCA axis 1 and second unconstrained DCA axis 2) was used to assess the influence an explanatory variable has in describing the variance in the chironomid community assemblage, and hence its predictive power (Juggins, 2013). All taxa were retained in the statistical analysis and rare taxa were down-weighted in the weighted average transfer function (down-weighting of rare species is implicit in the Bayesian approach). Multivariate analysis was carried out on square root transformed chironomid percentage data.

Inference models were developed using two separate approaches. The first method relied on weighted averaging methods, a tried and tested technique well established in quantitative palaeoecology (Birks, 1998; Birks *et al.*, 2012; ter Braak and Juggins, 1993; ter Braak and Looman, 1986). The second method uses a Bayesian approach, which in general has received less attention (Holden *et al.*, 2008). There are a number of inherent problems associated with quantitative inference models (Huntley, 2012; Juggins, 2013; Velle *et al.*, 2010) so the two independent methods were used to compare results and assess the strengths and weaknesses of each method.

The assemblage data was unimodal suggesting transfer functions using weighted averaging partial least squares (WA-PLS) were appropriate (ter Braak and Juggins, 1993). Inference models were also developed using classical and inverse weighted averaging (WA) to compare performance. The optimal number of components

frazer 2/26/2016 2:39 PM
Deleted: -
frazer 2/26/2016 2:39 PM
Formatted: Indent: First line: 0"
frazer 2/26/2016 2:41 PM
Formatted: Indent: First line: 0.25"

frazer 2/26/2016 2:41 PM
Deleted: -
frazer 2/25/2016 1:24 PM
Deleted: 3.4 Inference models -

frazer 2/25/2016 1:24 PM
Deleted: -
... [3]

259 was assessed using leave-one-out cross validation (jack knifing) and a minimum 5% change in prediction error
260 between components. Sample specific errors for the inferred temperatures were obtained through
261 bootstrapping 999 cycles.

262 Bayesian model selection was used to generate probability-weighted species response curves (SRCs) for
263 each taxon in the calibration dataset. Each taxon is assigned 8,000 possible SRCs. Each of these SRCs has a
264 probability weight based on its relative ability to describe the training data for that taxon. To perform a
265 reconstruction, likelihood functions (temperature probability distributions) are derived from each taxon in a
266 fossil sample, considering all 8,000 SRCs. Combining the likelihood functions of all the taxa in the fossil sample
267 derives the reconstruction. The power of the Bayesian approach is that it ascribes a probability distribution to
268 the reconstruction, providing a reconstruction-specific uncertainty. An important benefit is that all taxa in the
269 sample provide potentially useful information, even those with low counts that would be largely neglected in a
270 weighted averaging approach. To illustrate, a few counts of a taxon with a narrow temperature tolerance may
271 constrain the Bayesian reconstruction more than a very high count of a taxon with a broad tolerance.

272 Although the Bayesian model was developed for application to pH reconstructions from diatom
273 assemblages, it is generally applicable whenever it is appropriate to assume a unimodal species response to an
274 environmental gradient. The only modification required is the specification of appropriate priors. The *a priori*
275 probability distribution for optimum temperature in the SRCs was assigned to be uniform in the range -4.2 to
276 +30.8°C (training set range ± 5 C). The *a priori* probability for SRC tolerance was assigned to be uniform in the
277 range 2 to 10°C. Other SRC priors were unchanged from those in Holden *et al.* (2008).

278 DCCA detrending by segments, non-linear rescaling, and constrained by radiocarbon age was used to
279 determine compositional turnover constrained within the stratigraphic sequence (Birks and Birks, 2008). The
280 goodness-of-fit to temperature was evaluated by including the fossil chironomid samples passively in a CCA
281 ordination space of the modern training set samples constrained by MAT. Fossil samples with a squared residual
282 distance within the extreme 10% of the modern calibration dataset samples are considered as having a poor fit
283 to temperature. The modern analogue technique was used to test if fossil samples had good analogues within
284 the modern calibration data set. Any fossil sample with a squared chord distance larger than the 95% threshold
285 of the calibration data set is considered to have no good modern analogues (Birks, 1998; Velle *et al.*, 2005).

frazer 2/25/2016 1:24 PM

Formatted: Indent: First line: 0"

frazer 2/25/2016 1:24 PM

Deleted: -

... [4]

frazer 2/25/2016 1:24 PM

Deleted: -

... [5]

frazer 2/25/2016 2:06 PM

Formatted: Justified

290 Data were untransformed prior to analysing the dissimilarity using the modern analogue technique. The
291 significance of the final reconstruction was tested by comparing the amount of variance in the fossil data
292 explained by that reconstruction, compared with inferences produced by transfer functions trained on
293 randomly generated environmental data (Telford and Birks, 2011a). In this case, 999 random environmental
294 variables were generated in order to produce the null distribution.

295 4. Results

296 4.1 Calibration data set

297 The eight remaining explanatory variables, after those with VIFs >20 were removed; together explain
298 34.03% of the variance (Fig 3). The first two CCA axes explained 61.7% of the variance ($\lambda_1=0.792$, $\lambda_2 = 0.466$).
299 MAT describes most of the variance in the chironomid assemblages and has the highest $\lambda_1:\lambda_2$ ratio (Table 3).
300 When used as a single explanatory variable, MAT explains 12.93% of the variance ($\lambda_1/\lambda_2= 1.431$).

301 In total, 55 chironomid taxa were identified in the 59 training set lakes. *Chironomus anthracinus*-type was
302 the most widespread taxon, occurring over the entire temperature gradient (Fig 4). Orthoclaadiinae are generally
303 most abundant towards the cold end of the temperature gradient. *Cricotopus/Paratrichocladius* type III is the
304 dominant taxon of the coldest lake and is not present in sites >10°C MAT. Figure 4 shows the weighted average
305 and Bayesian optima and tolerance of each taxon ordered by lowest to highest optima as modelled in the
306 weighted averaging approach. In general the temperature optima predicted by each method are similar,
307 however, *Tanytarsus* type II and *Cricotopus/Paratrichocladius* type VII have colder optima when modelled using
308 a Bayesian approach. *Cricotopus/Paratrichocladius* type IV has the coldest temperature optimum, c. 3.3°C (Fig
309 5). Few Chironominae were found at the cold end of the calibration data set, but, for example, *Parachironomus*
310 and *Tanytarsus* type II were only found in lakes cooler than c. 8°C and had optima of c. 7.5°C and c. 6.5°C
311 respectively. *Paratanytarsus* and *Pseudosmittia* are important components of the chironomid assemblage
312 between 4-12°C, forming >50% of the chironomid community in some lakes, and have optima of c. 9.1 and 8.3°C
313 respectively. *Tanytarsus* type I, *Micropsectra* and *Einfeldia* are dominant taxa at mid-temperatures between c.
314 10-22°C. The absence of lakes between c. 16°C and c. 20°C limits a complete understanding of the distribution
315 of taxa occurring at these temperatures.

frazer 5/2/2016 4:49 PM

Deleted: Explanatory variables

frazer 2/26/2016 3:57 PM

Deleted: 2

frazer 2/26/2016 3:49 PM

Deleted: 2

frazer 5/2/2016 4:52 PM

Deleted: .

frazer 5/2/2016 4:52 PM

Deleted: 4.2 Calibration data set taxa .

frazer 5/2/2016 4:52 PM

Formatted: Add space between paragraphs of the same style

frazer 2/25/2016 2:22 PM

Deleted: (Matthews-Bird et al., 2015)

frazer 2/26/2016 3:56 PM

Deleted: 3

frazer 2/25/2016 2:22 PM

Deleted: (Matthews-Bird et al., 2015)

frazer 2/25/2016 2:24 PM

Deleted: a

frazer 2/26/2016 3:56 PM

Deleted: 4

326 DCCA analysis, constrained by MAT, indicates an assemblage shift across the temperature gradient of 2.2 SD
327 units. The biggest change in assemblage composition occurs above 12°C MAT (Fig 4). *Goeldichironomus*,
328 *Cladotanytarsus* and *Tanytarsus* type III were only found in lakes with MAT warmer than c. 22°C. Tanypodinae
329 were in greatest abundance at the warm end of the temperature gradient between c. 10-26°C, *Procladius* was
330 the most common Tanypodinae. It occurred between c. 10-26°C and had an optimum of c. 21°C.

331 Both methods (WA and Bayesian) produced similar performance statistics. The best performing model using
332 conventional statistical methods was a WA (inverse) model (Table 4, Fig 6)($R^2_{\text{jack}} = 0.890$, $\text{RMSEP}_{\text{jack}} = 2.404$ (°C),
333 Mean bias $_{\text{jack}} = -0.017$ (°C), Max bias $_{\text{jack}} = 4.665$ (°C)). The Bayesian method produced a slightly higher performing
334 model with $R^2_{\text{jack}} = 0.909$, $\text{RMSEP}_{\text{jack}} = 2.373$ (°C), Mean bias $_{\text{jack}} = 0.598$ (°C), Max bias $_{\text{jack}} = 3.158$ (°C).

336 4.2 Laguna Pindo fossil chironomids and dating

337 Chironomid remains were found only in the upper 416 cm of the 929cm sequence of Laguna Pindo (Fig 7).
338 In total, 2489 individual chironomid head capsules were analysed. The entire assemblage was made up of 32
339 taxa in 26 genera and 4 subfamilies. Among the taxa identified, 17 were Chironomini, eight Orthoclaadiinae and
340 three Tanypodinae. There was high variation between samples both in number of head capsules (average: 82;
341 range: 24 - 184) and concentration per gram of wet sediment (average: 73; range: 2 - 163). There was a marked
342 decline in head capsule concentration below 200 cm. In younger sediments (200-0 cm) head capsule
343 concentration averaged 106/gram, in older samples (200-420 cm) the average was 44/gram. Five zones were
344 identified using optimal partitioning with a broken stick model to define significant zones. *Polypedilum nubifer*-
345 type, *Procladius* and *Limnophyes* were the most abundant taxa; abundances are over 10% wherever they
346 occurred. *Tanytarsus* type II was most abundant below 200 cm (1500 cal yr BP) whilst *Polypedilum nubifer*-type
347 was present in low numbers below 340 cm (2300 cal yr BP). During periods of low *Polypedilum nubifer*-type
348 abundance, *Tanytarsus* type II and *Tanytarsus* type I occur in greater numbers (e.g. 420-360; 290-250 cm).

349 The best-fit age depth model for Laguna Pindo was a smooth spline (Fig 2). Due to the absence of
350 chironomids at the bottom of the sequence, six radiocarbon samples were used for building the model with a
351 total depth of the sediment considered of 461 cm (Table 2). The sedimentation rate ranged between 0.03 and

frazer 5/2/2016 4:52 PM

Formatted: Space After: 10 pt, Add space between paragraphs of the same

frazer 2/26/2016 3:56 PM

Deleted: 3

frazer 2/25/2016 2:29 PM

Moved down [1]: Chironomid larval head capsule concentrations can vary significantly between lakes, due to differences in preservation or abundance. Low counts can have adverse effects on the performance of inference models and the reliability of quantitative environmental reconstructions when using conventional methods (Heiri and Lotter, 2001; Quinlan and Smol, 2001). A minimum count size of 50 head capsules per sample is advised (Heiri and Lotter, 2001; Quinlan and Smol, 2001), however, good model performance has been achieved even when several samples include as few as 15-30 head capsules (Massaferro *et al.*, 2014). In some lakes in the current training set head capsule concentrations were as low as two head capsules per gram of sediment. Fifteen lakes in the data set produced fewer than 50 head capsules, and three lakes had fewer than 30. On average 77 individuals were analysed from each lake with a minimum count of 23 and a maximum of 164 (Table 1). Lakes with low head capsule counts were retained in the model in order to maintain as even coverage as possible across the temperature gradient.

frazer 5/2/2016 4:52 PM

Deleted: -

... [6]

frazer 5/2/2016 4:52 PM

Deleted: -

frazer 5/2/2016 4:52 PM

Formatted: Space After: 10 pt

frazer 2/26/2016 3:50 PM

Deleted: 3

frazer 2/26/2016 3:56 PM

Deleted: 5

frazer 2/26/2016 2:47 PM

Deleted: -

frazer 5/2/2016 4:52 PM

Deleted: 4

frazer 2/26/2016 3:55 PM

Deleted: 6

frazer 2/26/2016 4:00 PM

Deleted: 51

frazer 2/26/2016 4:00 PM

Deleted: 51

387 0.5 cm/yr, with a sampling interval resolution of 97 years between samples on average (range from 27 to 196
388 years).

389 4.3 Palaeotemperature reconstruction

390 Both transfer functions (WA inverse and Bayesian) show similar patterns in the temperature
391 reconstruction (Fig 8). From 3000-2500 cal yr BP inferred temperatures are cold relative to the modern (20.2°C).
392 The minimum WA inverse temperatures are much colder (13.5°C±2.5) than the inferred Bayesian temperatures
393 (17.5°C±3.7) for the early section of the sequence. From 2400 to 1700 cal yr BP inferred temperatures from
394 both methods oscillate around c. 18-19°C but remained depressed relative to the modern. A notable feature of
395 both reconstructions is the sudden drop in inferred temperatures at 1600 cal yr BP. Inferred temperatures fall
396 by c. 2°C to 17.5°C±2.7. This abrupt drop in temperature is short-lived in both reconstructions and temperatures
397 return to previous values in the subsequent sample. From 1500 cal yr BP to the present the chironomid-inferred
398 temperatures stabilise and steadily rise. Peak temperatures for the entire record (21.9°C±3.5) are inferred
399 between 400-700 cal yr BP. Temperatures begin to cool from 400 cal yrs BP in both reconstructions, reaching a
400 minimum of c. 17°C±2.5 c. 100 cal yr BP before rising rapidly to between 20-21°C±2.5 in the most recent
401 sediment sample. On average the Bayesian model infers warmer temperatures than the WA model.

402 The fossil samples of Laguna Pindo plot within the modern variation of chironomid assemblages when
403 included passively in a CCA analysis of the calibration data set (Fig 9). This suggests that the calibration dataset
404 is appropriate for the fossil sequence of Laguna Pindo. The fossil samples plot along the MAP gradient
405 suggesting precipitation is an important variable controlling the variance in the fossil assemblages. The sites
406 associated with high precipitation in the calibration dataset are located in the same region of the Ecuadorian
407 Andes as the fossil site. With a modern MAT of c. 20°C, however, Laguna Pindo is located in a region of the
408 temperature gradient that is poorly covered in the calibration dataset (Fig 4). Seven taxa found in the Laguna
409 Pindo sequence do not occur in any of the analysed calibration data set lakes. These include three unknown
410 morphotypes, three *Xestochironomus* morphotypes, and *Metriocnemus eurynotus*-type. These taxa, however,
411 never comprise more than 10% of the chironomid assemblage of any one sample.

412 Fourteen of the fossil samples are considered to have a poor goodness-of-fit to temperature and all
413 fossil samples are considered as having poor modern analogues in the calibration data set (Fig 10). Although the

frazer 5/2/2016 4:52 PM

Deleted: 5

frazer 2/26/2016 3:55 PM

Deleted: 7

frazer 2/26/2016 3:55 PM

Deleted: 8

frazer 2/26/2016 3:56 PM

Deleted: 3

frazer 2/25/2016 1:06 PM

Deleted: ,

frazer 2/25/2016 1:06 PM

Deleted: although the samples plot within the range of modern calibration lakes that lie at similar elevations (1000-3000 m a.s.l.).

frazer 2/25/2016 2:56 PM

Deleted: Seven

frazer 2/26/2016 3:54 PM

Deleted: 9

424 modern analogue technique is not used to infer past temperatures the lack of modern analogues in the fossil
425 assemblage is important when considering the reliability of any reconstruction.

426 DCCA constrained by radiocarbon age shows an abrupt change at 1475 cal yr BP between zones 3 and 4
427 and a turnover of 1.6 SD units over the whole sequence (Fig 10). Much of the variation in goodness-of-fit and
428 DCCA sample scores is mirrored by changes in count size and head capsule concentration. The sudden drop in
429 head capsule concentration occurs at a step change in DCCA assemblage variation (1475 cal yrs BP) (Fig 10).
430 Periods of increased count size and head capsule concentration in older sediments (2100-2250 cal yrs BP) also
431 coincides with periods of improved goodness-of-fit (Fig 10). The WA classical inferred MAT values using the
432 modern calibration data set explain more of the variance than 95% of randomly generated variables and so the
433 WA classical MAT reconstructions can be deemed statistically significant ($p= 0.032$) (Fig 11) (Telford and Birks,
434 2011a).

435

436 5. Discussion

437 5.1 Chironomids and environmental variables

438 Chironomids have been shown to respond to temperature at a variety of spatial scales and taxonomic levels
439 (Brooks, 2006; Eggermont and Heiri, 2011). Temperature is a key variable in controlling chironomid
440 development at all stages of their life cycles, and influences voltinism, behaviour and metabolism (Armitage *et*
441 *al.*, 1995). Across the Northern Hemisphere, over large temperature gradients, mean July air temperature, the
442 warmest month of the year, which reflects the developmental period of most species, has been shown to be the
443 major determinant of variation in chironomid assemblages (Brooks, 2006; Walker and Cwynar, 2006). As a
444 result, many quantitative temperature inference models have been developed to reconstruct mean July air
445 temperature. Across the tropics however seasonal variation is small and many chironomids are multivoltine
446 (Walker and Mathews, 1987) so temperatures throughout the year are likely to be relatively more influential. In
447 tropical East Africa, Eggermont *et al.* (2010) demonstrated that mean annual air temperature was a significant
448 driver of chironomid assemblage composition and developed a chironomid-based inference model on this basis.
449 Similarly, Wu *et al.* (2014) showed MAT to be the most important environmental variable when developing a
450 chironomid inference model for Central America. When attempting to make quantitative inferences from fossil

frazer 2/26/2016 3:55 PM

Deleted: 9

frazer 2/26/2016 2:50 PM

Deleted: The most recent sample is clearly distinct from any other period of the record.

frazer 2/26/2016 3:55 PM

Deleted: 9

frazer 2/26/2016 3:55 PM

Deleted: 9

frazer 2/26/2016 3:54 PM

Deleted: 0

457 assemblages it is first crucial to establish that the variable of interest is an important ecological determinant.
458 The variable to be reconstructed must describe a statistically important component of the variance within the
459 assemblage data (Juggins, 2013). Compared to other measured variables, mean annual temperature explained
460 the largest amount of chironomid assemblage variance and had the highest eigenvalue ratio ($\lambda_1:\lambda_2$) in the
461 Andean calibration dataset (Table 3). The explanatory strength of temperature in the calibration data set meets
462 the minimum criterion proposed by Juggins (2013) (i.e. $\lambda_1:\lambda_2 > 1.0$) for temperature being a suitable variable to
463 reconstruct from this calibration dataset.

464 The DCCA results suggest that precipitation is also a strong ecological determinant ($\lambda_1:\lambda_2=0.9$); the
465 passive plot of fossil samples with calibration samples further supports this conclusion. The fossil samples of
466 Laguna Pindo are strongly associated with MAP. Precipitation in Andean landscapes, however, is spatially
467 heterogeneous and geographically close localities experience significantly different rainfall patterns (Garreaud
468 *et al.*, 2009). Lakes associated with high rainfall (Fig 3) are actually in areas of the northern Andes with two rainy
469 seasons a year. It is very likely that the bimodality of rainfall in these areas is as important in controlling
470 chironomid populations as the total amount of rainfall as measured by MAP. Precipitation is also intrinsically
471 linked to temperature as both temperature and precipitation increase with decreasing latitude in tropical South
472 America (Garreaud *et al.*, 2009). Unlike temperature, precipitation affects chironomids indirectly making any
473 quantitative inference difficult. Precipitation will alter a suite of environmental variables (e.g. pH, conductivity,
474 depth, substrate) making quantitative inferences of precipitation problematic. As chironomid life cycles are
475 strongly controlled by temperature and many tropical chironomid species tend to be multivoltine, we suggest
476 the most appropriate variable both ecologically and statistically to reconstruct using the Andean calibration
477 data sets is MAT although the of influence of precipitation cannot be overlooked.

478 The optima and temperature tolerances (Fig 5) of many taxa found in the current study are similar to
479 that noted in other Neotropical chironomid calibration datasets, further supporting the conclusion of
480 temperature being an important ecological determinant. For example, Wu *et al.* (2014) in Central America,
481 found taxa of the genera *Beardius*, *Labrundinia* and *Goeldichironomus* to have optima between 23-24°C whilst
482 *Limnophyes* and *Corynoneura* where more abundant at the colder end of the gradient with optima of 15°C and
483 18°C respectively. In the current dataset *Beardius*, *Labrundinia*, and *Goeldichironomus* all have optima between

frazer 2/26/2016 3:49 PM
Deleted: 2

frazer 2/26/2016 3:57 PM
Deleted: 2

frazer 2/26/2016 3:56 PM
Deleted: 4

487 23-24°C and *Limnophyes* and taxa of *Corynoneura* also have optima of 15°C and 19°C, respectively. *Limnophyes*
488 also has one of the broadest tolerances of all taxa in both calibration datasets suggesting the genus is probably
489 represented by many species (Matthews-Bird et al., 2015). More work is needed in order to refine chironomid
490 larval taxonomy in South America, however the current data suggest the potential for a larger calibration
491 dataset applicable to wider area incorporating the Northern Neotropics and Central America.

492

493 5.2 Model performance

494 Although both models (WA inverse and Bayesian) perform well (WA RMSEP= 2.4°C/9.6% of training set
495 range and Bayesian RMSEP= 2.3°C/9.2% of training set range), some of the best performing chironomid-based
496 temperature inference models have prediction errors closer to 1.0°C (Brooks and Birks, 2001; Heiri et al., 2011,
497 2007; Olander et al., 1999). The highest performing chironomid inference models often have in excess of 100-
498 150 calibration sites compared with just 59 in the current model and this may account for its reduced
499 performance. Furthermore the lakes in the calibration data set are not evenly distributed over the temperature
500 gradient. The cold end of the gradient has a higher number of lakes (34 cold, high elevation lakes) than at warm
501 and intermediate temperatures (15 warm, mid-low elevation lakes). Uneven sampling has been shown to lead
502 to biases which may reduce RMSEP (Telford and Birks, 2011b). Furthermore the over-representation of cold
503 lakes in the current dataset may result in under-estimation of the temperature optima of some taxa and,
504 therefore, bias temperature estimates towards cold values. In the Andean dataset, as analysis of residuals
505 shows, temperatures around 10°C are often under-estimated (Fig 6). Furthermore, the inferred temperatures of
506 Laguna Pindo are on average cooler than the modern day conditions.

507 The absence of lakes in part of the temperature gradient may limit the reliability of estimates of optima
508 and tolerances of taxa and also create 'edge effects' in the middle of the temperature range, in addition to
509 those that occur at the cold and warm end of the temperature gradient (Eggermont et al., 2010). Such problems
510 are inherent to WA models as predicted values are pulled towards the mean of the training set resulting in
511 under- and over-estimations of high and low values (ter Braak and Juggins 1993). However, despite having no
512 lakes between 16-20°C in the calibration data set, additional edge effects are not a feature of the current

frazer 2/26/2016 3:56 PM

Deleted: 5

514 inference model. The gap of c. 4°C does not appear to have compromised model performance, probably as the
515 interval is not significant and taxa have tolerances that span these temperatures.

516 Chironomid larval head capsule concentrations can vary significantly between lakes, due to differences in
517 preservation or abundance. Low counts can have adverse effects on the performance of inference models and
518 the reliability of quantitative environmental reconstructions when using conventional methods (Heiri and
519 Lotter, 2001; Quinlan and Smol, 2001). A minimum count size of 50 head capsules per sample is advised (Heiri
520 and Lotter, 2001; Quinlan and Smol, 2001), however, good model performance has been achieved even when
521 several samples include as few as 15-30 head capsules (Massafiero *et al.*, 2014). In some lakes in the current
522 training set head capsule concentrations were as low as two head capsules per gram of sediment. Fifteen lakes
523 in the data set produced fewer than 50 head capsules, and three lakes had fewer than 30. On average 77
524 individuals were analysed from each lake with a minimum count of 23 and a maximum of 164 (Table 1). Lakes
525 with low head capsule counts were retained in the model in order to maintain as even coverage as possible
526 across the temperature gradient.

527
528 *Polypedilum nubifer*-type and *Chironomus anthracinus*-type make up a large component of the
529 chironomid assemblages in lakes across the entire temperature gradient (Fig 4). Such eurythermic taxa probably
530 include several different species. It is difficult to model reliable, or even meaningful, optima for eurythermic
531 taxa. Poor model performance or unreliable reconstructions may result if the assemblage is dominated by
532 eurythermic taxa. We note that eurythermic taxa are described by high tolerance SRCs in the Bayesian
533 approach, leading to increased uncertainty in reconstructions through broad likelihood functions that
534 contribute little information to the posterior. Inferred temperature of c. 10°C, are likely to be underestimated as
535 many taxa found at these temperatures also occur in cold lakes, which are over-represented in the calibration
536 data-set. In African lakes Eggermont *et al.* (2010) found that the presence of eurythermic taxa such as
537 *Chironomus* type Kibos caused an overestimation of temperatures in lakes at the warm end of the gradient.
538 They also found that the occurrence of *Limnophyes minimus*-type and *Paraphaenocladus* type OI Bolossat
539 overestimated the temperature of lakes close to where gaps occurred in the gradient (Eggermont *et al.*, 2010).
540 Similarly, in a New Zealand calibration data set developed by Woodward and Shulmeister (2006), *Chironomus*

frazer 2/25/2016 2:29 PM
Moved (insertion) [1]

frazer 2/26/2016 3:56 PM
Deleted: 3

542 was present in both high elevation, cold, oligotrophic lakes and lower elevation, warm, eutrophic lakes. The
543 intermediate temperature optimum estimated for this taxon resulted in over-estimated temperatures of cold
544 lakes and under-estimates of warm lakes (Woodward and Shulmeister, 2006). Eurythermic taxa may be
545 contributing to the over-estimation of cold temperatures and the under-estimation of temperatures in the
546 middle of the gradient in the Andean inference model.

547

548 5.3 WA vs Bayesian

549 Despite similar performance statistics between the Bayesian and WA methods, the inferred pattern of late-
550 Holocene temperature change is different. Temperatures inferred c. 2700 cal yr BP (400 cm) (Fig 8) using the
551 WA inverse method is extremely cold (c. 14°C) compared with the rest of the record. This reconstruction is
552 driven by the high abundance of *Tanytarsus* type II, a taxon that has a WA temperature optimum of 6.5°C. The
553 Bayesian reconstruction for this sample of 17.8 ±2.8°C, is in line with more modest temperature shifts that
554 would be expected in the late-Holocene (Wanner *et al.*, 2008). One advantage of the Bayesian methodology is
555 the transparency of the reconstruction through consideration of individual likelihood functions for this
556 assemblage (Fig 12). Although *Tanytarsus* type II is abundant in the sample its influence in the reconstruction is
557 moderated by several other taxa with higher temperature optima that are present at low abundances. This
558 temperature estimate demonstrates the Bayesian reconstruction can be sensitive to a few counts of a species
559 that have a negligible effect in a WA approach. The likelihood function for Chironomini type II, which has an
560 abundance of only 2.3% in the sample, constrains the reconstruction more than *Tanytarsus* type II, which has an
561 abundance of 74%. This is because Chironomini type II is only found in the warmest lakes in the calibration set, each
562 time with a low abundance. We note that because it is found in only three training set sites, Chironomini type II is
563 associated with many (671) high-probability SRCs, defined as having a probability great that 10% of the most likely
564 SRC. For this reason, its likelihood function is relatively broad and extends to temperatures far lower than the
565 temperature of the sites in which the taxon is found in the training set.

566

567 5.4 Temperature and secondary environmental variables

frazer 2/26/2016 3:55 PM
Deleted: 7

frazer 2/26/2016 3:54 PM
Deleted: 1

frazer 2/26/2016 3:01 PM
Deleted: -

frazer 2/26/2016 3:01 PM
Deleted: 5

573 Whilst the λ_1/λ_2 of 1.431 indicates that MAT is appropriate for reconstruction using this calibration dataset
574 (Juggins, 2013), it does not necessarily mean that reliable temperature reconstructions can be obtained from a
575 fossil record (Telford and Birks, 2011a). Before attempting to interpret any reconstruction several metrics can
576 be used to assess the validity of a reconstruction (Juggins and Telford, 2012).

577 The modern analogue technique compares the similarity of the fossil samples to the modern samples in the
578 calibration data set. All fossil samples are greater than the 5th percentile of the square chord distance (Fig 10),
579 which suggests there is no close modern analogue in the calibration set to any fossil sample (Birks, 1998; Juggins
580 and Birks, 2001). The lack of modern analogues in the Laguna Pindo fossil sequence is due to the many taxa
581 present in the fossil samples that are not present in the calibration data set. This may reflect the lack of lakes in
582 the calibration dataset with MAT values close to those of Laguna Pindo. Nevertheless, WA and WAPLS models
583 have been shown to perform well in non-analogue situations (Birks *et al.*, 2010). The Bayesian method
584 generates temperature reconstructions from likelihood functions of species in the calibration data set. Although
585 analogous assemblages are not required for the Bayesian reconstruction (each taxon is treated equally and
586 individually), species that are absent from the training set cannot contribute information to the posterior,
587 thereby increasing the uncertainty associated with the reconstruction. One advantage of the Bayesian
588 methodology is that this uncertainty is explicitly incorporated into the Bayesian reconstruction (Holden *et al.*,
589 2008).

590 During periods of poor fit-to-temperature, variables other than temperature may have been affecting the
591 composition of the chironomid assemblage. As noted previously, the CCA biplot of fossil samples included
592 passively with the significant explanatory variables (Fig 9) shows that MAP was also important in driving the
593 assemblage variance. During times of poor fit to temperature the influence of precipitation as a secondary
594 variable may be more important than temperature in influencing the chironomid assemblage composition.
595 Indeed, precipitation has been shown to be an important variable in controlling the modern distribution of
596 chironomid taxa in the tropical Andes (Matthews-Bird *et al.*, 2015).

597 Samples with poor fit-to-temperature also corresponded with samples having low numbers of head
598 capsules. The number of head capsules retrieved will directly affect how representative a sample is to the
599 chironomid fauna (Heiri, 2004; Quinlan and Smol, 2001). The cold oscillations inferred from the Bayesian

frazer 2/26/2016 3:54 PM

Deleted: 9

frazer 2/26/2016 3:55 PM

Deleted: 8

602 reconstruction are more in line with what is expected during the late-Holocene (1-3°C); the likelihood functions
603 of rare species, which favour warm conditions, combine to rule out the anomalously cold temperatures
604 suggested by some of the WA reconstructions. As discussed above, the over-representation of cold lakes in the
605 calibration dataset will likely bias species optima to colder values in a weighted average approach so there may
606 be a tendency for the model to underestimate temperature, especially during cold periods. This problem is
607 likely exaggerated when head capsule concentration is low, cold indicator taxa may have higher abundances
608 than would be the case if all taxa were accurately represented.

609 The DCCA results indicate that there was a distinct change in the composition of the chironomid
610 assemblage after 1600 cal yr BP (210 cm). This largely coincides with an increase in head capsule concentration,
611 possibly indicating an increase in lake productivity, and the shift in chironomid-inferred temperatures from low
612 to high. Indeed post 1600 cal yr BP, (210 cm) samples are inferred as being on average 2-3°C warmer than early
613 sections using Bayesian and WA models respectively.

614 Although the temperature reconstruction has a good ecological basis, because chironomids globally are
615 highly sensitive to temperature and Laguna Pindo is on an ecotonal boundary that is sensitive to temperature
616 changes, precipitation is influential as a secondary variable. The WA inverse MAT reconstruction, however, is
617 statistically significant based on the criteria described by Telford and Birks (2011a) (Fig 11) suggesting that
618 despite precipitation as a possible confounding variable, a temperature signal can be obtained from Neotropical
619 chironomids. We would caution, however, against an over interpretation at this stage. Due to some of the
620 limitations discussed previously, the reconstruction can only currently be deemed qualitative and requires more
621 research before quantitative estimates can be generated with confidence.

frazer 2/26/2016 3:54 PM

Deleted: 0

622

623 6. Conclusions

624 The chironomid fauna of the tropical Andes have been shown to be sensitive to climate variables,
625 particularly temperature and precipitation. Both variables (MAT and MAP) meet the basic criteria for being used
626 in an environmental reconstruction using the Andean calibration dataset. MAT, however, is an important
627 determinant of chironomid species distribution and abundance and was therefore more appropriate to be

frazer 2/26/2016 3:11 PM

Formatted: Indent: First line: 0"

frazer 2/26/2016 3:11 PM

Deleted: 5.6 Cooling climate 3800-2800 ca' ... [8]

631 reconstructed. The influence of precipitation should be explored further and must be considered as an
632 important secondary variable especially when reconstructing past conditions in the region. It is very likely that
633 the influence of precipitation noted here relates to the annual variability in rainfall across the Andes as opposed
634 to overall amount making any quantitative interpretations even more difficult.

635 The two techniques used to develop inference models (WA and Bayesian) show comparable performance
636 statistics (WA inverse model $R^2_{\text{jack}} = 0.890$, $\text{RMSEP}_{\text{jack}} = 2.404(^{\circ}\text{C})$, $\text{Mean bias}_{\text{jack}} = -0.017(^{\circ}\text{C})$, $\text{Max bias}_{\text{jack}} = 4.665(^{\circ}\text{C})$;
637 Bayesian model $R^2_{\text{jack}} = 0.909$, $\text{RMSEP}_{\text{jack}} = 2.373(^{\circ}\text{C})$, $\text{Mean bias}_{\text{jack}} = 0.598(^{\circ}\text{C})$, $\text{Max bias}_{\text{jack}} = 3.158(^{\circ}\text{C})$). This work demonstrates a proof of method, however, a larger calibration dataset with a more even
638 coverage of calibration sites is needed in order to improve model performance. The Bayesian approach
639 provided a transparent reconstruction less susceptible to the effect of an uneven distribution of calibration sites
640 and performed particularly well during periods of low count size and when inferring cold intervals. The
641 chironomid-based MAT reconstruction from the Laguna Pindo is often colder than would be expected for
642 Holocene timescales. The underestimated temperatures are most likely the direct result of an over
643 representation of cold lakes in the calibration dataset. The addition of more calibration sites between 12°C and
644 20°C would expand our understanding of tropical Andean chironomid distribution, and significantly improve
645 model performance and reconstruction reliability.

647 Knowledge of past tropical climate dynamics is fundamental not only to understanding regional climate
648 but also global climate patterns and hemispherical teleconnections. Quantitative temperature proxies, such as
649 chironomids, will provide valuable data on past climate variability in the region. The reconstructions presented
650 here demonstrate the potential of the proxy and also highlights the complexity of late-Holocene climate change
651 in tropical South America.

652

653

654 **Acknowledgements**

frazer 2/26/2016 3:07 PM

Deleted: fossil record suggests that periods of low solar output not only affect the tropics through changes in precipitation, but also directly affect tropical temperatures. Inferred temperatures were 2-3°C cooler relative to the modern during the widely recognised 3500-2500 cal yr BP cooling event. Long-term cooling during the late Holocene is not apparent in the Laguna Pindo record. However, temperatures do cool by 1-2.2°C relative to the modern during the LIA period, although this is only noted in a single fossil sample.

666 Funding was provided by the Natural Environment Research Council (NERC), UK. NERC grant (ref:
667 NE/J018562/1) was awarded to E. Montoya and (ref: NE/J500288/1) awarded to F. Matthews-Bird. This work
668 was supported by the NERC Radiocarbon Facility NRCF010001 (allocation number 1682.1112). Special thanks to
669 Dr Pauline Gulliver for her continuous involvement and support during radiocarbon dating. The authors also
670 wish to thank Mark Bush, Francis Mayle, Yarrow Axford, Alex Chepstow-Lusty and Mick Frogley for their kind
671 donation of samples. [Data is stored with the National Geoscience Data Centre \(NGDC\) and can be found at](http://www.bgs.ac.uk/downloads/home.html)
672 <http://www.bgs.ac.uk/downloads/home.html>.

673

674

675 References

- 676 Alley, R.B., 2000. The Younger Dryas cold interval as viewed from central Greenland. *Quat. Sci. Rev.* 19, 213–
677 226.
- 678 Anderson, E.D., 1997. Younger Dryas research and its implications for understanding abrupt climatic change.
679 *Prog. Phys. Geogr.* 21, 230–249.
- 680 Armitage, P.D., Cranston, P.S., Pinder, L.C.V., 1995. *The Chironomidae: the biology and ecology of nonbiting*
681 *midges*. London: Chapman and Hall.
- 682 Baker, P. a., Fritz, S.C., 2015b. Nature and causes of Quaternary climate variation of tropical South America.
683 *Quat. Sci. Rev.* 124, 31–47. doi:10.1016/j.quascirev.2015.06.011
- 684 Baker, P.A., Seltzer, G.O., Fritz, S.C., Dunbar, R.B., Grove, M.J., Tapia, P.M., Cross, S.L., Rowe, H.D., Broda, J.P.,
685 2001. The history of South American tropical precipitation for the past 25,000 years. *Science* 291, 640–
686 643. doi:10.1126/science.291.5504.640
- 687 Bird, B.W., Abbott, M.B., Vuille, M., Rodbell, D.T., Stansell, N.D., Rosenmeier, M.F., 2011. A 2,300-year-long
688 annually resolved record of the South American summer monsoon from the Peruvian Andes. *Proc. Natl.*
689 *Acad. Sci. U. S. A.* 108, 8583–8. doi:10.1073/pnas.1003719108
- 690 Birks, H.J.B., 1998. Numerical tools in palaeolimnology—Progress, potentialities and problems. *J. Paleolimnol.* 20,
691 307–332.
- 692 Birks, H.J.B., Birks, H.H., 2008. Biological responses to rapid climate change at the Younger Dryas–Holocene
693 transition at Krakenes, western Norway. *The Holocene* 18, 19–30. doi:10.1177/0959683607085572
- 694 Birks, H.J.B., Heiri, O., Seppä, H., Bjune, A.E., 2010. Strengths and Weaknesses of Quantitative Climate
695 Reconstructions Based on Late-Quaternary Biological Proxies. *Open Ecol. J.* 3, 68–110.
- 696 Birks, H.J.B., Lotter, A.F., Juggins, S., Smol, J.P. (Eds.), 2012. *Tracking Environmental Change Using Lake*
697 *Sediments; Data Handling and Numerical Techniques*. Springer Netherlands.
- 698 Blaauw, M., 2010. Methods and code for “classical” age-modelling of radiocarbon sequences. *Quat.*
699 *Geochronol.* 5, 512–518. doi:10.1016/j.quageo.2010.01.002
- 700 Brooks, S.J., 2006. Fossil midges (Diptera: Chironomidae) as palaeoclimatic indicators for the Eurasian region.
701 *Quat. Sci. Rev.* 25, 1894–1910. doi:10.1016/j.quascirev.2005.03.021

frazer 2/25/2016 3:28 PM

Deleted: Baker, P. a., Fritz, S.C., 2015a. Nature and causes of Quaternary climate variation of tropical South America. *Quat. Sci. Rev.* 124, 31–47. doi:10.1016/j.quascirev.2015.06.011

frazer 2/25/2016 3:29 PM

Deleted: -

- 707 Brooks, S.J., 2000. Chironomid-inferred Late-glacial air temperatures at Whitrig Bog, Southeast Scotland. *J.*
708 *Quat. Sci.* 15, 759–764.
- 709 Brooks, S.J., Axford, Y., Heiri, O., Langdon, P.G., Larocque-Tobler, I., 2012. Chironomids can be reliable proxies
710 for Holocene temperatures. A comment on Velle et al. (2010). *The Holocene* 22, 1495–1500.
711 doi:10.1177/0959683612449757
- 712 Brooks, S.J., Birks, H.J.B., 2001. Chironomid-inferred air temperatures from Lateglacial and Holocene sites in
713 north-west Europe: progress and problems. *Quat. Sci. Rev.* 20, 1723–1741. doi:10.1016/S0277-
714 3791(01)00038-5
- 715 Brooks, S.J., Birks, H.J.B., 2000. Chironomid-inferred late-glacial and early-Holocene mean July air temperatures
716 for Kråkenes Lake, western Norway. *J. Paleolimnol.* 23, 77–89.
- 717 Brooks, S.J., Langdon, P.G., 2014. Summer temperature gradients in northwest Europe during the Lateglacial to
718 early Holocene transition (15–8 ka BP) inferred from chironomid assemblages. *Quat. Int.* 1–11.
719 doi:10.1016/j.quaint.2014.01.034
- 720 Brooks, S.J., Langdon, P.G., Heiri, O., 2007. The Identification and use of Palaeartic Chironomidae Larvae in
721 Palaeoecology. QRA Technical Guide No. 10, Quaternary Research Association, London.
- 722 Čiamporová-Zařovířová, Z., Hamerlík, L., Šporka, F., Bitušík, P., 2010. Littoral benthic macroinvertebrates of
723 alpine lakes (Tatra Mts) along an altitudinal gradient: a basis for climate change assessment. *Hydrobiologia*
724 648, 19–34. doi:10.1007/s10750-010-0139-5
- 725 Colinvaux, P., De Oliveira, P.E., Patino, J.E., 1999. Amazon Pollen Manual and Atlas. Harwood Academic
726 Publishers.
- 727 Collins, M., An, S.-I., Cai, W., Ganachaud, A., Guilyardi, E., Jin, F.-F., Jochum, M., Lengaigne, M., Power, S.,
728 Timmermann, A., Vecchi, G., Wittenberg, A., 2010. The impact of global warming on the tropical Pacific
729 Ocean and El Niño. *Nat. Geosci.* 3, 391–397. doi:10.1038/ngeo868
- 730 Cranston, P.S., 2010. URL <http://chirokey.skullisland.info/>.
- 731 Crowley, T.J., 2000. Causes of Climate Change Over the Past 1000 Years. *Science*, 289, 270–277.
732 doi:10.1126/science.289.5477.270
- 733 Dimitriadis, S., Cranston, P.S., 2001. An Australian Holocene climate reconstruction using Chironomidae from a
734 tropical volcanic maar lake. *Palaeogeogr. Palaeoclimatol. Palaeoecol.* 176, 109–131.
- 735 Eggermont, H., Heiri, O., 2011. The chironomid-temperature relationship: expression in nature and
736 palaeoenvironmental implications. *Biol. Rev. Camb. Philos. Soc.* 87, 430–456. doi:10.1111/j.1469-
737 185X.2011.00206.x
- 738 Eggermont, H., Heiri, O., Russell, J., Vuille, M., Audenaert, L., Verschuren, D., 2010. Paleotemperature
739 reconstruction in tropical Africa using fossil Chironomidae (Insecta: Diptera). *J. Paleolimnol.* 43, 413–435.
740 doi:10.1007/s10933-009-9339-2
- 741 Epler, J.H., 2001. Identification manual for the Larval Chironomidae (Diptera) of South Carolina.
- 742 Frey, D.G., 1988. Littoral and offshore communities of diatoms, cladocerans and dipterous larvae, and their
743 interpretation in paleolimnology. *J. Paleolimnol.* 1, 179–191.
- 744 Garreaud, R.D., Vuille, M., Compagnucci, R., Marengo, J., 2009. Present-day South American climate.
745 *Palaeogeogr. Palaeoclimatol. Palaeoecol.* 281, 180–195. doi:10.1016/j.palaeo.2007.10.032
- 746 Hastenrath, S., 2012. Climate dynamics of the tropics. Springer Science & Business Media.
- 747 Haug, G.H., Hughen, K.A., Sigman, D.M., Peterson, L.C., Röhl, U., 2001. Southward migration of the intertropical
748 convergence zone through the Holocene. *Science* 293, 1304–8. doi:10.1126/science.1059725
- 749 Heiri, O., 2004. Within-lake variability of subfossil chironomid assemblages in shallow Norwegian lakes. *J.*
750 *Paleolimnol.* 32, 67–84. doi:10.1023/B:JOPL.0000025289.30038.e9
- 751 Heiri, O., Brooks, S.J., Birks, H.J.B., Lotter, A.F., 2011. A 274-lake calibration data-set and inference model for
752 chironomid-based summer air temperature reconstruction in Europe. *Quat. Sci. Rev.* 30, 3445–3456.

frazer 2/25/2016 3:30 PM

Deleted: No Title [WWW Document].

frazer 2/25/2016 3:30 PM

Deleted: (80-.)

- 755 doi:10.1016/j.quascirev.2011.09.006
- 756 Heiri, O., Brooks, S.J., Renssen, H., Bedford, A., Hazekamp, M., Ilyashuk, B., Jeffers, E.S., Lang, B., Kirilova, E.,
757 Kuiper, S., Millet, L., Samartin, S., Toth, M., Verbruggen, F., Watson, J.E., van Asch, N., Lammertsma, E.,
758 Amon, L., Birks, H.H., Birks, H.J.B., Mortensen, M.F., Hoek, W.Z., Magyari, E., Muñoz Sobrino, C., Seppä, H.,
759 Tinner, W., Tonkov, S., Veski, S., Lotter, A.F., 2014. Validation of climate model-inferred regional
760 temperature change for late-glacial Europe. *Nat. Commun.* 5, 4914. doi:10.1038/ncomms5914
- 761 Heiri, O., Cremer, H., Engels, S., Hoek, W.Z., Peeters, W., Lotter, A.F., 2007. Lateglacial summer temperatures in
762 the Northwest European lowlands: a chironomid record from Hijkermeer, the Netherlands. *Quat. Sci. Rev.*
763 26, 2420–2437. doi:10.1016/j.quascirev.2007.06.017
- 764 Heiri, O., Lotter, A., 2001. Effect of low count sums on quantitative environmental reconstructions: an example
765 using subfossil chironomids. *J. Paleolimnol.* 26, 343–350.
- 766 Heiri, O., Lotter, A.F., Hausmann, S., Kienast, F., 2003. A chironomid-based Holocene summer air temperature
767 reconstruction from the Swiss Alps. *The Holocene* 13, 477–484.
- 768 Heiri, O., Lotter, A.F., Lemke, G., 2001. Loss on ignition as a method for estimating organic and carbonate
769 content in sediments: reproducibility and comparability of results. *J. Paleolimnol.* 25, 101–110.
- 770 Hijmans, R.J., Cameron, S.E., Parra, J.L., Jones, P.G., Jarvis, A., 2005. Very high resolution interpolated climate
771 surfaces for global land areas. *Int. J. Climatol.* 25, 1965–1978. doi:10.1002/joc.1276
- 772 Hill, M., Gauch, H., 1980. Detrended correspondence analysis: an improved ordination technique. *Vegetatio* 42,
773 47–58.
- 774 Hogg, A.G., Hua, Q., Blackwell, P.G., Niu, M., Buck, C.E., Guilderson, T.P., Heaton, T.J., Palmer, J.G., Reimer, P.J.,
775 Reimer, R.W., Turney, C.S.M., Zimmerman, S.R.H., 2013. SHCal13 Southern Hemisphere calibration, 0–
776 50,000 cal yr BP. *Radiocarbon* 55, 1889–1903.
- 777 Holden, P.B., Mackay, A.W., Simpson, G.L., 2008. A Bayesian palaeoenvironmental transfer function model for
778 acidified lakes. *J. Paleolimnol.* 39, 551–566. doi:10.1007/s10933-007-9129-7
- 779 Huntley, B., 2012. Reconstructing palaeoclimates from biological proxies: Some often overlooked sources of
780 uncertainty. *Quat. Sci. Rev.* 31, 1–16. doi:10.1016/j.quascirev.2011.11.006
- 781 Ivanochko, T., Ganeshram, R., Brummer, G., Ganssen, G., Jung, S., Moreton, S., Kroon, D., 2005. Variations in
782 tropical convection as an amplifier of global climate change at the millennial scale. *Earth Planet. Sci. Lett.*
783 235, 302–314. doi:10.1016/j.epsl.2005.04.002
- 784 Jansen, E., Overpeck, J., Briffa, K., Duplessy, J.-C., Joos, F., Masson-Delmotte, V., Olago, D., Otto-Bliesner, B.,
785 Peltier, W., Rahmstorf, S., Ramesh, R., Raynaud, D., Rind, O., Solomina, O., Villalba, R., Zhang, D., 2007.
786 *Climate Change 2007: The Physical Science Basis. Contribution of Working Group I to the Fourth*
787 *Assessment Report of the Intergovernmental Panel on Climate Change*, in: Solomon, S., Qin, D., Manning,
788 M., Chen, Z., Marquis, M., Averyt, K.B., Tignor, M., Miller, H. (Eds.), . Cambridge University Press,
789 Cambridge, United Kingdom and New York, NY, USA.
- 790 Johnsen, S.J., Dahl-Jensen, D., Gundestrup, N., Steffensen, J.P., Clausen, H.B., Miller, H., Masson-Delmotte, V.,
791 Sveinbjörnsdóttir, A.E., White, J., 2001. Oxygen isotope and palaeotemperature records from six
792 Greenland ice-core stations: Camp Century, Dye-3, GRIP, GISP2, Renland and NorthGRIP. *J. Quat. Sci.* 16,
793 299–307. doi:10.1002/jqs.622
- 794 Jomelli, V., Favier, V., Rabatel, A., Brunstein, D., Hoffmann, G., Francou, B., 2009. Fluctuations of glaciers in the
795 tropical Andes over the last millennium and palaeoclimatic implications: A review. *Palaeogeogr.*
796 *Palaeoclimatol. Palaeoecol.* 281, 269–282. doi:10.1016/j.palaeo.2008.10.033
- 797 Jones, P., Mann, M., 2004. Climate over past millennia. *Rev. Geophys.* 42, 1–42.
798 doi:10.1029/2003RG000143.CONTENTENTS
- 799 Juggins, S., 2013. Quantitative reconstructions in palaeolimnology: new paradigm or sick science? *Quat. Sci. Rev.*
800 64, 20–32. doi:10.1016/j.quascirev.2012.12.014
- 801 Juggins, S., Birks, H.J.B., 2001. Quantitative Environmental Reconstructions from Biological Data, in: Birks, H.J.B.,

frazer 2/25/2016 3:32 PM

Deleted: e

803 Lotter, A.F., Juggins, S., Smol, J.P. (Eds.), Tracking Environmental Change Using Lake Sediments,
804 Developments in Paleoenvironmental Research 5. pp. 431–494.

805 Juggins, S., Telford, R.J., 2012. Exploratory Data Analysis and Data Display, in: Birks, H.J.B., Lotter, A.F., Juggins,
806 S., Smol, J.P. (Eds.), Tracking Environmental Change Using Lake Sediments, Developments in
807 Paleoenvironmental Research 5, Developments in Paleoenvironmental Research. Springer Netherlands,
808 Dordrecht, pp. 123–141. doi:10.1007/978-94-007-2745-8

809 Kanner, L.C., Burns, S.J., Cheng, H., Edwards, R.L., Vuille, M., 2013. High-resolution variability of the South
810 American summer monsoon over the last seven millennia: insights from a speleothem record from the
811 central Peruvian Andes. *Quat. Sci. Rev.* 75, 1–10. doi:10.1016/j.quascirev.2013.05.008

812 Leng, M.J., Marshall, J.D., 2004. Palaeoclimate interpretation of stable isotope data from lake sediment
813 archives. *Quat. Sci. Rev.* 23, 811–831. doi:10.1016/j.quascirev.2003.06.012

814 Marcott, S. a, Shakun, J.D., Clark, P.U., Mix, A.C., 2013. A reconstruction of regional and global temperature for
815 the past 11,300 years. *Science* 339, 1198–1201. doi:10.1126/science.1228026

816 Markgraf, V., 1989. Palaeoclimates in Central and South America since 18,000 BP based on Pollen and lake-level
817 records. *Quat. Sci. Rev.* 8, 1–24.

818 Massaferro, J., Larocque, I.T., 2013. Using a newly developed chironomid transfer function for reconstructing
819 mean annual air temperature at Lake Potrok Aike, Patagonia, Argentina. *Ecol. Indic.* 24, 201–210.
820 doi:10.1016/j.ecolind.2012.06.017

821 Massaferro, J., Larocque-Tobler, I., Brooks, S.J., Vandergoes, M., Dieffenbacher-Krall, A., Moreno, P., 2014.
822 Quantifying climate change in Huelmo mire (Chile, Northwestern Patagonia) during the Last Glacial
823 Termination using a newly developed chironomid-based temperature model. *Palaeogeogr. Palaeoclimatol.*
824 *Palaeoecol.* 399, 214–224. doi:10.1016/j.palaeo.2014.01.013

825 Matthews-Bird, F., Gosling, W.D., Coe, A.L., Bush, M., Mayle, F.E., Axford, Y., Brooks, S.J., 2015. Environmental
826 controls on the distribution and diversity of lentic Chironomidae (Insecta : Diptera) across an altitudinal
827 gradient in tropical South America. *Ecol. Evol.* 1–22. doi:10.1002/ece3.1833

828 Mayewski, P.A., Rohling, E.E., Curt Stager, J., Karlén, W., Maasch, K.A., David Meeker, L., Meyerson, E. a., Gasse,
829 F., van Kreveland, S., Holmgren, K., Lee-Thorp, J., Rosqvist, G., Rack, F., Staubwasser, M., Schneider, R.R.,
830 Steig, E.J., 2004. Holocene climate variability. *Quat. Res.* 62, 243–255. doi:10.1016/j.yqres.2004.07.001

831 Meyer, I., Wagner, S., 2008. The Little Ice Age in southern Patagonia : Comparison between paleoecological
832 reconstructions and downscaled model output of a GCM simulation. *PAGES news* 16.

833 Mosblech, N. a. S., Bush, M.B., Gosling, W.D., Hodell, D., Thomas, L., van Calsteren, P., Correa-Metrio, A.,
834 Valencia, B.G., Curtis, J., van Woesik, R., 2012. North Atlantic forcing of Amazonian precipitation during the
835 last ice age. *Nat. Geosci.* 5, 817–820. doi:10.1038/ngeo1588

836 O'Brien, S.R., Mayewski, P. a., Meeker, L.D., Meese, D.A., Twickler, M.S., Whitlow, S.I., 1995. Complexity of
837 Holocene Climate as Reconstructed from a Greenland Ice Core. *Science* (80-.). 270, 1962–1964.

838 Olander, H., Korhola, a., Blom, T., Birks, H.J.B., 1999a. An expanded calibration model for inferring lakewater
839 and air temperatures from fossil chironomid assemblages in northern Fennoscandia. *The Holocene* 9, 279–
840 294. doi:10.1191/095968399677918040

841 Olander, H., Korhola, a., Blom, T., Birks, H.J.B., 1999b. An expanded calibration model for inferring lakewater
842 and air temperatures from fossil chironomid assemblages in northern Fennoscandia. *The Holocene* 9, 279–
843 294. doi:10.1191/095968399677918040

844 Oldfield, F., Steffen, W., 2014. Anthropogenic climate change and the nature of Earth System science. *Anthr.*
845 *Rev.* 1, 70–75. doi:10.1177/2053019613514862

846 Pinder, L.C.V., 1986. Biology of freshwater Chironomidae. *Annu. Rev. Entomol.* 31, 1–23.

847 Polissar, P.J., Abbott, M.B., Wolfe, a P., Bezada, M., Rull, V., Bradley, R.S., 2006. Solar modulation of Little Ice
848 Age climate in the tropical Andes. *Proc. Natl. Acad. Sci. U. S. A.* 103, 8937–42.
849 doi:10.1073/pnas.0603118103

850 Prat, N., Rieradevall, M., Acosta, R., Villamarín, C., M, G.D.I.F.E., 2011. Las Larvas de Chironomidae (Diptera) DE
851 Los rios Altoandinos de Ecuador y Peru, Clave par la determinacion de los generos.

852 Quinlan, R., Smol, J., 2001. Setting minimum head capsule abundance and taxa deletion criteria in chironomid-
853 based inference models. *J. Paleolimnol.* 26, 327–342.

854 Rees, A.B.H., Cwynar, L.C., Cranston, P.S., 2008. Midges (Chironomidae, Ceratopogonidae, Chaoboridae) as a
855 temperature proxy: a training set from Tasmania, Australia. *J. Paleolimnol.* doi:10.1007/s10933-008-9222-
856 6

857 Reuter, J., Stott, L., Khider, D., Sinha, A., Cheng, H., Edwards, R.L., 2009. A new perspective on the hydroclimate
858 variability in northern South America during the Little Ice Age. *Geophys. Res. Lett.* 36, L21706.
859 doi:10.1029/2009GL041051

860 Rieradevall, M., Brooks, S., 2001. An identification guide to subfossil Tanypodinae larvae (Insecta: Diptera:
861 Chironomidae) based on cephalic setation. *J. Paleolimnol.* 81–99.

862 Self, A.E., Brooks, S.J., Birks, H.J.B., Nazarova, L., Porinchu, D., Odland, A., Yang, H., Jones, V.J., 2011. The
863 distribution and abundance of chironomids in high-latitude Eurasian lakes with respect to temperature
864 and continentality: development and application of new chironomid-based climate-inference models in
865 northern Russia. *Quat. Sci. Rev.* 30, 1122–1141. doi:10.1016/j.quascirev.2011.01.022

866 Telford, Birks, H.J.B., 2011a. A novel method for assessing the statistical significance of quantitative
867 reconstructions inferred from biotic assemblages. *Quat. Sci. Rev.* 30, 1272–1278.
868 doi:10.1016/j.quascirev.2011.03.002

869 Telford, Birks, H.J.B., 2011b. Effect of uneven sampling along an environmental gradient on transfer-function
870 performance. *J. Paleolimnol.* 46, 99–106. doi:10.1007/s10933-011-9523-z

871 ter Braak, C.J.F., 1987. Ordination, in: Jongman, R., ter Braak, C.J., van Tongeren, O.F.R. (Eds.), *Data Analysis in
872 Community Ecology*. Pudoc, Wageningen, The Netherlands, pp. 91–173.

873 ter Braak, C.J.F., Juggins, S., 1993. Weighted averaging partial least squares regression (WA-PLS): an improved
874 method for reconstructing environmental variables from species assemblages. *Hydrobiologia* 269/70, 485–
875 502.

876 ter Braak, C.J.F., Looman, C.W., 1986. Weighted averaging, logisitic regression and the Gaussian response
877 model. *Vegetatio* 65, 3–11.

878 Thompson, L., Mosley-Thompson, E., Dansgaard, W., Grootes, P., 1986. The Little Ice Age as Recorded in the
879 Stratigraphy of the Tropical Quelccaya Ice Cap. *Science*, 234, 361–364.

880 Thompson, L.G., Mosley-Thompson, E., Brecher, H., Davis, M., León, B., Les, D., Lin, P.-N., Mashiotta, T.,
881 Mountain, K., 2006. Abrupt tropical climate change: past and present. *Proc. Natl. Acad. Sci. U. S. A.* 103,
882 10536–43. doi:10.1073/pnas.0603900103

883 Thompson, L.G., Mosley-Thompson, E., Davis, M.E., 1995. Late glacial stage and Holocene tropical ice core
884 records from Huascan, Peru. *Science*, 269, 46–50.

885 Thompson, L.G., Mosley-Thompson, E., Davis, M.E., Henderson, K.A., Brecher, H.H., Zagorodnov, V.S.,
886 Mashiotta, T.A., Lin, P.-N., Mikhalenko, V.N., Hardy, D.R., Beer, J., 2002. Kilimanjaro ice core records:
887 evidence of Holocene climate change in tropical Africa. *Science* 298, 589–93. doi:10.1126/science.1073198

888 Trivinho-Strixino, S., 2011. Larvas de Chironomidae guia de Identificacao. Universidade Federale de Sao Carlos.

889 van Geel, B., Raspopov, O.M., Renssen, H., Plicht, J. Van Der, Dergachev, V.A., Meijer, H.A.J., 1999. The role of
890 solar forcing upon climate change. *Quat. Sci. Rev.* 18, 331–338.

891 Velle, G., Brodersen, K.P., Birks, H.J.B., Willassen, E., 2010. Midges as quantitative temperature indicator
892 species: Lessons for palaeoecology. *The Holocene* 20, 989–1002. doi:10.1177/0959683610365933

893 Velle, G., Brooks, S.J., Birks, H.J.B., Willassen, E., 2005. Chironomids as a tool for inferring Holocene climate: an
894 assessment based on six sites in southern Scandinavia. *Quat. Sci. Rev.* 24, 1429–1462.
895 doi:10.1016/j.quascirev.2004.10.010

896 Vuille, M., Bradley, R., Keimig, F., 2000. Climate variability in the Andes of Ecuador and its relation to tropical

frazer 2/25/2016 3:33 PM

Deleted: (80-.)

frazer 2/25/2016 3:32 PM

Deleted: (80-.)

frazer 2/25/2016 3:34 PM

Deleted: h

frazer 2/25/2016 3:33 PM

Deleted: Thompson, L.G., Mosley-Thompson, E., Davis, M.E., Lin, P.N., Henderson, K.A., Cole-Dai, J., Bolzan, J.F., Liu, K.B., 1995. Late glacial stage and holocene tropical ice core records from huascan, peru. *Science* 269, 46–50. doi:10.1126/science.269.5220.46 .

906 Pacific and Atlantic sea surface temperature anomalies. *J. Clim.* 13, 2520–2535.

907 Walker, I.R., Cwynar, L.C., 2006. Midges and palaeotemperature reconstruction—the North American
 908 experience. *Quat. Sci. Rev.* 25, 1911–1925. doi:10.1016/j.quascirev.2006.01.014

909 Walker, I.R., Mathews, R.W., 1987. Chironomids, lake trophic status and climate. *Quat. Res.* 28, 431–437.

910 Wanner, H., Beer, J., Bütikofer, J., Crowley, T.J., Cubasch, U., Flückiger, J., Goosse, H., Grosjean, M., Joos, F.,
 911 Kaplan, J.O., Küttel, M., Müller, S.A., Prentice, I.C., Solomina, O., Stocker, T.F., Tarasov, P., Wagner, M.,
 912 Widmann, M., 2008. Mid- to Late Holocene climate change: an overview. *Quat. Sci. Rev.* 27, 1791–1828.
 913 doi:10.1016/j.quascirev.2008.06.013

914 Wiederholm, T., 1983. Chironomid of the Holarctic region. Keys and diagnosis. Part 1. Larvae. *Entomologica
 915 Scandinavica Supplement* 19.

916 Woodward, C., Shulmeister, J., 2006. New Zealand chironomids as proxies for human-induced and natural
 917 environmental change: transfer functions for temperature and lake production (chlorophyll a). *J.
 918 Paleolimnol.* 36, 407–429.

919 Wu, J., Porinchu, D.F., Horn, S.P., Haberyan, K. a., 2014. The modern distribution of chironomid sub-fossils
 920 (Insecta: Diptera) in Costa Rica and the development of a regional chironomid-based temperature
 921 inference model. *Hydrobiologia* 742, 107–127. doi:10.1007/s10750-014-1970-x

922

923

924

925

926

927

928

929

930

931

932

933

934

935

936

937

938

frazer 2/25/2016 3:34 PM
 Deleted: .

940 **Table captions**

941 **Table 1**

942 Summary of the physical and chemical properties of the 59 calibration data set lakes including the total number
943 of head capsules retrieved from each lake and the concentration of head capsules per gram of sediment. MAT=
944 mean annual temperature, MAP= mean annual precipitation, LOI=loss-on-ignition (550°C).

945 **Table 2**

946 AMS radiocarbon dates used for the age-depth model of Lake Pindo. SUERC: lab code (from NERC Radiocarbon
947 Facility, East Kilbride); BS: Bulk sediment; W: Wood; WA: weighted average.

949 **Table 3**

950 Results of detrended canonical correspondence analysis (DCCA) using single constraining variables. MAT= mean
951 annual temperature, WT=water temperature, MAP=mean annual precipitation, LOI= Loss-on-ignition.

952 **Table 4**

953 Summary of the performance statistics of chironomid-based MAT(°C) inference models developed using
954 classical and Bayesian methods based on leave one out cross validation. Weighted averaging inverse and
955 classical (WAINV, WAcla), Weighted averaging partial least squares (WA-PLS), coefficient of determinant
956 between predicted and observed (r^2_{jack}), root mean squared error of prediction (RMSEP_{jack}) as % of the gradient.

957

958

959

960

961

962

963

frazer 2/26/2016 3:47 PM
Deleted: -
frazer 2/26/2016 3:40 PM
Formatted: Font:+Theme Body
frazer 2/26/2016 3:39 PM
Deleted: 1

frazer 2/26/2016 3:39 PM
Deleted: 2

frazer 2/26/2016 3:40 PM
Deleted: 3

frazer 2/26/2016 3:47 PM
Deleted: -
frazer 2/26/2016 3:47 PM
Formatted: Indent: Left: 0", First line: 0"

969

970

971

Tables

Table 1

	Calibration data set				
	Minimum	Mean	Median	Maximum	Std dev
Conductivity (μ s)	5.9	363	185	3205	579
Depth (m)	0.1	5	2.2	25	5.4
Elevation (m a.s.l)	150	3142	3845	4655	1459
Latitude (S)	0.1	11.2	14.2	17.3	6.2
Longitude (W)	64.4	71.6	70.3	78.4	4.5
LOI (%)	0	19	13	80	16
MAT ($^{\circ}$ C)	0.8	12	10	25	7
MAP (mm/year)	468	1222	769	4421	952
pH	5.7	8	7.9	10.2	1.1
Total Head Capsules	23	77	76	164	35
Water Temperature ($^{\circ}$ C)	5	15	13	33	6
Head capsule/gram	2	27	22	105	22

frazer 2/26/2016 3:47 PM
 Deleted: ... [9]
 frazer 2/26/2016 3:47 PM
 Formatted: Centered

972

973

Table 2

Sample code	Depth (cm)	Sample type	Age (yr 14 C BP)	Age (cal yrs BP) 2σ	Age (cal yr BP) estimation (WA)
SUERC-54395	46	W	334 \pm 42	289-470	373
SUERC-47634	117	W	974 \pm 36	769-923	835
SUERC-47635	245	W	1973 \pm 39	1812-1943	1868
SUERC-47569	329	W	2335 \pm 37	2293-2361	2279
SUERC-47572	410	W	2829 \pm 39	2781-2991	2916
SUERC-48854	461	BS	3974 \pm 45	4241-4447	4336

frazer 3/24/2016 10:04 AM
 Comment [1]: Table added after reviewer suggestion

974

975

976

frazer 2/26/2016 3:48 PM
 Formatted: Indent: Left: 0", First line: 0"

977

Table 3

Variable	Variance Explained (%)	λ_1/λ_2	P
MAT	12.93	1.431	0.001
MAP	10.3	0.900	0.001
WT	11.21	1.230	0.001
pH	6.23	0.500	0.001
LOI	3.23	0.239	0.062
Depth	2.44	0.190	0.240
Conductivity	2.34	0.179	0.296

frazer 2/26/2016 3:41 PM
 Deleted: 2

978

979

980

981

982

986
987
988
989

990
991
992
993
994
995
996
997
998
999
000
001
002
003
004
005

Table 4

Model	R ² _{Jack}	RMSEP _{Jack}	Mean bias _{Jack}	Max bias _{Jack}	% change
WA (inv)	0.890	2.404	-0.017	4.665	-
WA (cla)	0.890	2.475	-0.035	4.279	-2.936
WA-TOL (inv)	0.851	2.831	-0.182	6.498	-
WA-TOL (cla)	0.852	2.951	-0.211	7.350	-4.263
WA-PLS (1)	0.889	2.431	0.094	4.891	-
WA-PLS (2)	0.890	2.412	0.109	3.982	0.766
WA-PLS (3)	0.869	2.617	0.096	5.558	-8.483
WA-PLS (4)	0.866	2.659	0.199	5.922	-1.592
WA-PLS (5)	0.875	2.568	0.213	6.201	3.409
Bayesian	0.909	2.373	0.598	3.158	

frazer 2/26/2016 3:41 PM
Deleted: 3

frazer 2/26/2016 3:47 PM
Deleted: -

Figure captions

Figure 1

Location of the calibration data set lakes (black circles) and Laguna Pindo (white triangle).

Figure 2

Sediment description, radiocarbon dates (¹⁴C age) and age-depth models of Laguna Pindo. Key colour for sediment descriptions: Black or dark brown = organic rich sediments (peat and clay respectively); White = dark sandy intervals; Greenish = greenish sandy clay, not compacted; Yellow = sediment gap (no sediment).

frazer 2/26/2016 3:43 PM
Formatted: Line spacing: double

Figure 3

Figure 2: Canonical correspondence analysis (CCA) of the calibration data set lakes and environmental variables with elevation and longitude removed after variance inflation analysis. MAP=mean annual precipitation, MAT=mean annual temperature, WT= water temperature, LOI=loss-on-ignition. Grey circles denote calibration lakes, dark grey triangles mark species. All species could not be labelled due to crowding; instead nine important taxa have been marked as examples.

frazer 2/26/2016 3:43 PM
Deleted: 2

Figure 4

Chironomid taxa in the modern calibration dataset lakes. Lakes are ordered (top to bottom) from cold to warm and chironomids are ordered by occurrence from cold to warm lakes. Only taxa present in three or more lakes are included. Dashed line shows a gap in calibration data set lakes between 16-20 °C of the MAT gradient. Detrended canonical correspondence analysis (DCCA) constrained by MAT shows the taxon turnover across the gradient. Head capsule concentration (hc/gram) is also included.

frazer 2/26/2016 3:43 PM
Deleted: 3

Figure 5

Weighted-average and Bayesian optima (solid grey circles) and tolerances (thick lines) of the 55-chironomid taxa included in the calibration dataset, MAT Range (dashed lines). Taxa are organised by WA temperature optima from cold to warm.

frazer 2/26/2016 3:43 PM
Deleted: 4

Figure 6

frazer 2/26/2016 3:43 PM
Deleted: 5

036 Model performance of the best performing classical method (WA) and Bayesian approach. A=weighted
037 averaging method; B=Bayesian method. WA: $R^2_{jack} = 0.890$, $RMSEP_{jack} = 2.404^{\circ}C$, $Mean\ bias_{jack} = -0.017^{\circ}C$, $Max\ bias_{jack} = 4.665^{\circ}C$. Bayesian: $R^2_{jack} = 0.909$, $RMSEP_{jack} = 2.373^{\circ}C$, $Mean\ bias_{jack} = 0.598^{\circ}C$, $Max\ bias_{jack} = 3.158^{\circ}C$.

frazer 2/25/2016 3:37 PM
Formatted: Font:+Theme Body, 11 pt
frazer 2/26/2016 3:43 PM
Deleted: .

039 **Figure 7**
040 Diagram of fossil chironomid assemblage of Laguna Pindo. Five significant zones were identified using optimal
041 partitioning with a broken stick model. Detrended canonical correspondence analysis (DCCA) constrained by
042 calibrated radiocarbon age shows taxon turnover through time. Only taxa with relative abundances greater
043 than 5% are shown. SD=standard deviation, hc/gram= head capsules per gram of wet sediment.

frazer 2/26/2016 3:43 PM
Deleted: 6

044 **Figure 8**
045 Chironomid-inferred mean annual temperatures (MAT) at Laguna Pindo using the WA inverse (grey) and
046 Bayesian (black) models. Sample specific errors for the WA model are obtained through bootstrapping 999
047 cycles. Errors of the Bayesian reconstruction are site-specific uncertainties.

frazer 2/26/2016 3:43 PM
Deleted: 7

048 **Figure 9**
049 Distribution of Laguna Pindo fossil samples (black circles) included passively within a CCA of the calibration data
050 set lakes (grey circles) constrained using the significant environmental variables. MAP= mean annual
051 precipitation, MAT= mean annual temperature, WT= water temperature. The first and last fossil sample in the
052 sedimentary sequence has been labelled (total sediment depth); there are no directional trends through time.

frazer 3/24/2016 9:38 AM
Deleted: Key late-Holocene climate events are shaded in grey. LIA=the range of the earliest and latest date for the Little Ice Age in South America (Polissar *et al.*, 2006). 3500-2500 global cooling event (Mayewski *et al.*, 2004), note, however, the Laguna Pindo record only extends to 3000 cal yrs BP.

frazer 2/26/2016 3:43 PM
Deleted: 8

frazer 2/26/2016 3:43 PM
Formatted: Justified, Indent: Left: 0", First line: 0", Line spacing: double

053 Calibration lakes that lie at similar elevations as Laguna Pindo have been labelled.

frazer 2/26/2016 3:43 PM
Deleted: [10]

054 **Figure 10**
055 (left to right): Chironomid-inferred WA classical MAT with sample specific errors generated using bootstrapping.
056 Bayesian reconstruction with sample specific errors. Goodness-of-fit of the fossil assemblages to temperature,
057 vertical dotted line indicates the 90th percentile of squared residual distances of modern samples to first axis in
058 a CCA; samples to the right of the line have a poor fit-to-temperature. Nearest modern analogue analysis,
059 vertical dotted line indicates the 5th percentile of squared chord distances of the fossil samples in the modern
060 calibration data set; samples to the right of the line have no good modern analogues. Detrended canonical

frazer 2/26/2016 3:43 PM
Deleted: 9

075 correspondence analysis (DCCA) sample scores with radiocarbon age used as the sole constraining variable.
076 Head capsule concentration per gram of sediment. Zones are derived from optimal partitioning of fossil
077 assemblages using a broken stick model to define significant zones. Sq res dis= square residual distance; Sq chrd
078 dis= square chord distance; SD units= standard deviation units; hc/gram=head capsule per gram of sediment.

079 **Figure 11**

080 Histogram of the proportion of variance in the chironomid MAT transfer function explained by 999 transfer
081 functions trained on random environmental variables. Solid black line denotes the proportion of variance
082 explained by the chironomid WA inverse MAT transfer function. Black dashed line marks the proportion of
083 variance explained by the first axis of PCA of the fossil data. Grey dashed line marks the 95% variance of the
084 random reconstructions.

frazer 2/26/2016 3:43 PM
Deleted: 0

085 **Figure 12**

086 Individual likelihood functions for the fossil taxa in the coldest sample of the Laguna Pindo sequence (396 cm
087 total depth, c. 2700 cal yr BP). The posterior probability distribution for temperature for the fossil sample is
088 plotted in red, note this is plotted on an independent axis.

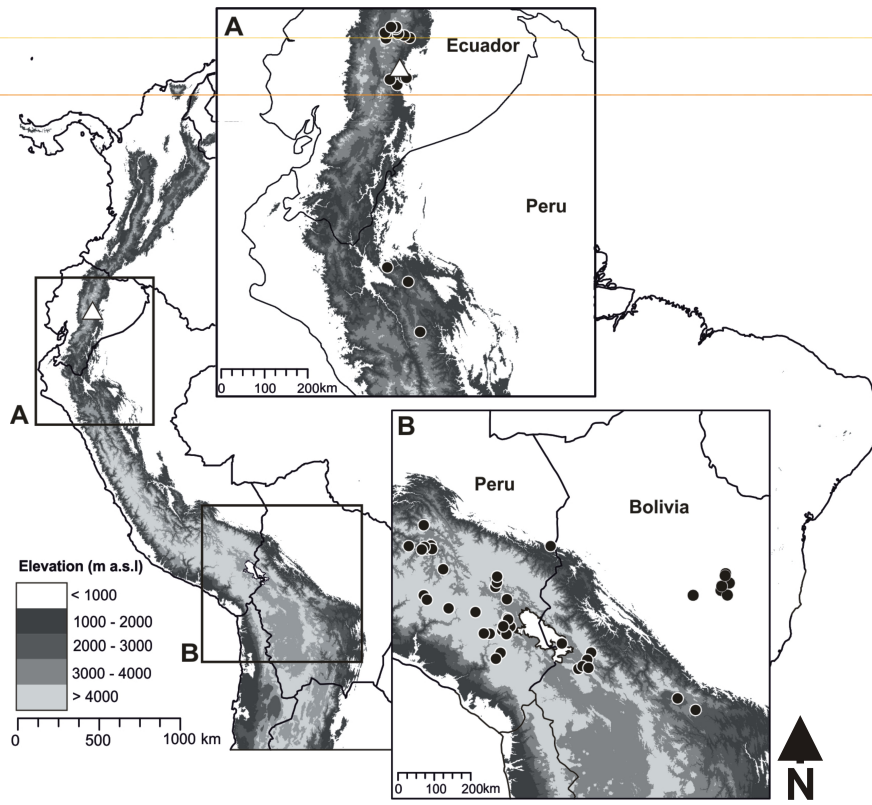
frazer 2/26/2016 3:43 PM
Deleted: 1

089
090
091
092
093
094
095
096
097

Figures

frazer 2/26/2016 3:43 PM
Deleted: - ... [11]

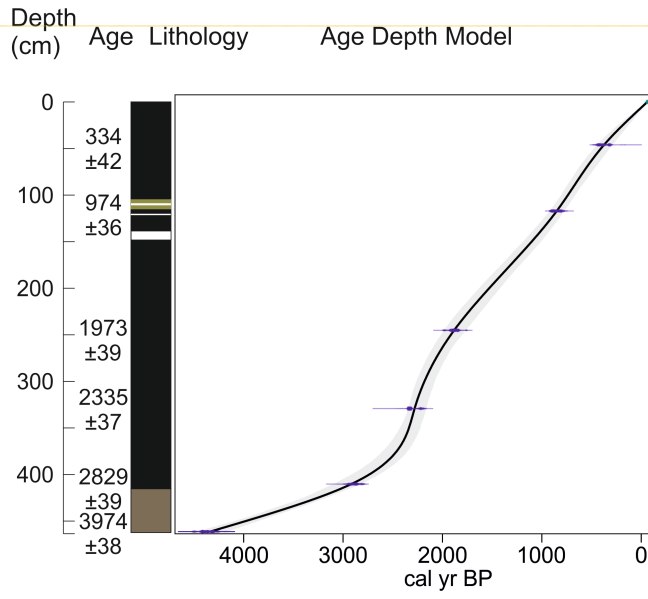
102 **Figure 1**



- 103 frazer 3/24/2016 10:05 AM
- 104 **Comment [2]:** North arrow added
- 105 Unknown
- 106 **Formatted:** Font:Calibri, Bold
- 107 frazer 2/26/2016 2:14 PM
- 108 **Deleted:** <sp>
- 109 Unknown
- 110 **Formatted:** Font:Bold

128
129
130
131
132
133
134
135
136
137
138
139
140
141
142
143
144
145
146
147
148
149
150
151
152

Figure 2



frazer 3/24/2016 10:05 AM
Comment [3]: Figure removed from supplementary and included in the manuscript

Unknown
Formatted: Font:Bold

153 **Figure 3**

154

155

156

157

158

159

160

161

162

163

164

165

166

167

168

169

170

171

172

173

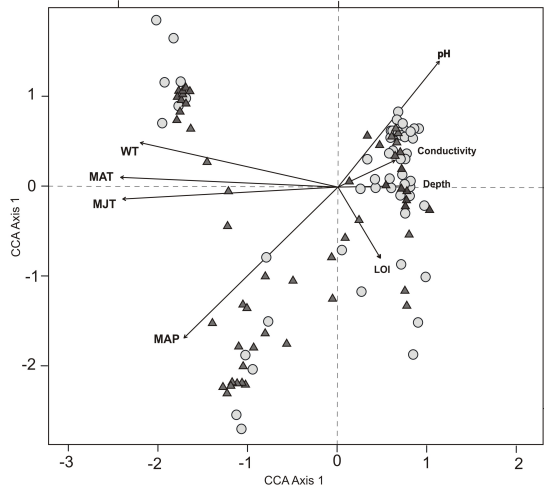
174

175

176

177

178



frazer 3/24/2016 10:06 AM

Comment [4]: Latitude removed from the analysis

frazer 2/26/2016 3:44 PM

Deleted: 2

frazer 2/26/2016 2:15 PM

Deleted: <sp>

Unknown

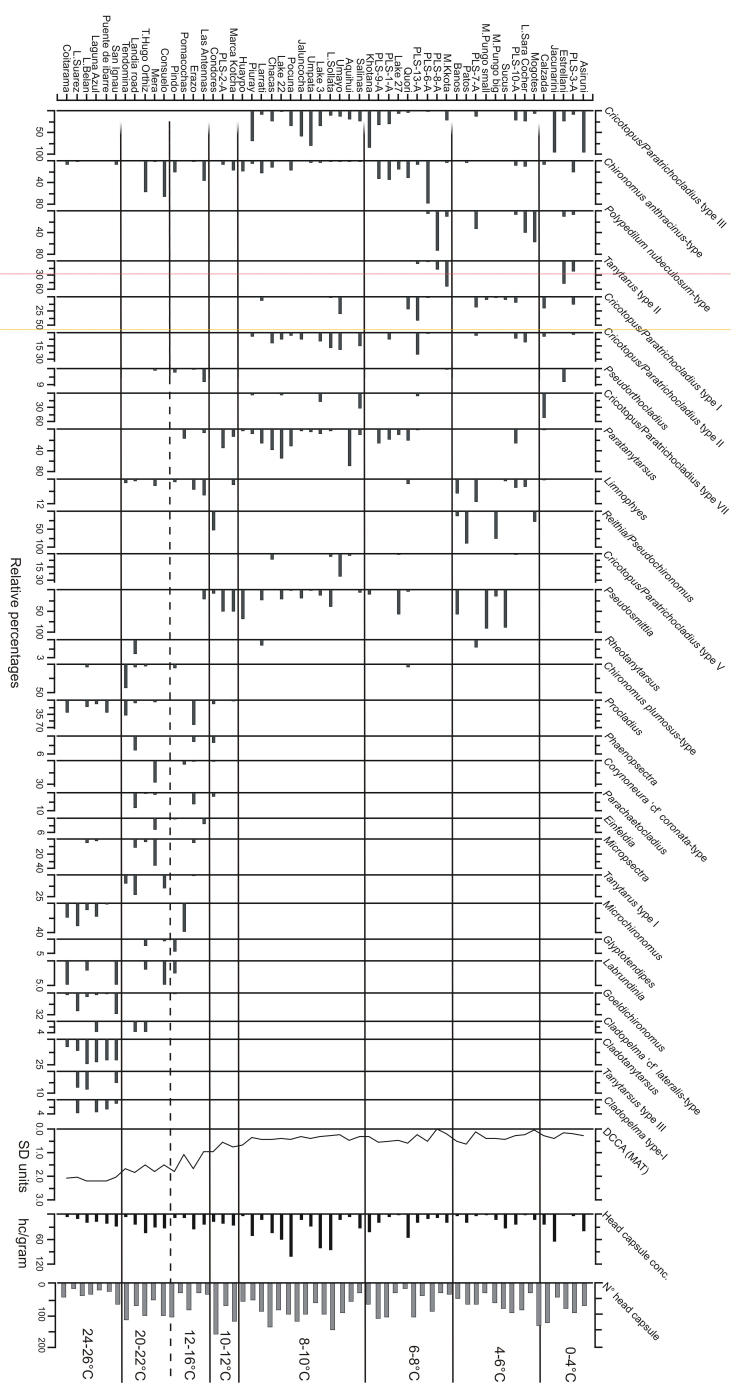
Formatted: Font:Calibri

Unknown

Formatted: Font:Bold

181
182
183
184
185
186
187
188
189
190
191
192
193
194
195
196
197
198
199
200
201
202
203
204
205
206

Figure 4



frazer 2/26/2016 3:44 PM
Deleted: 3

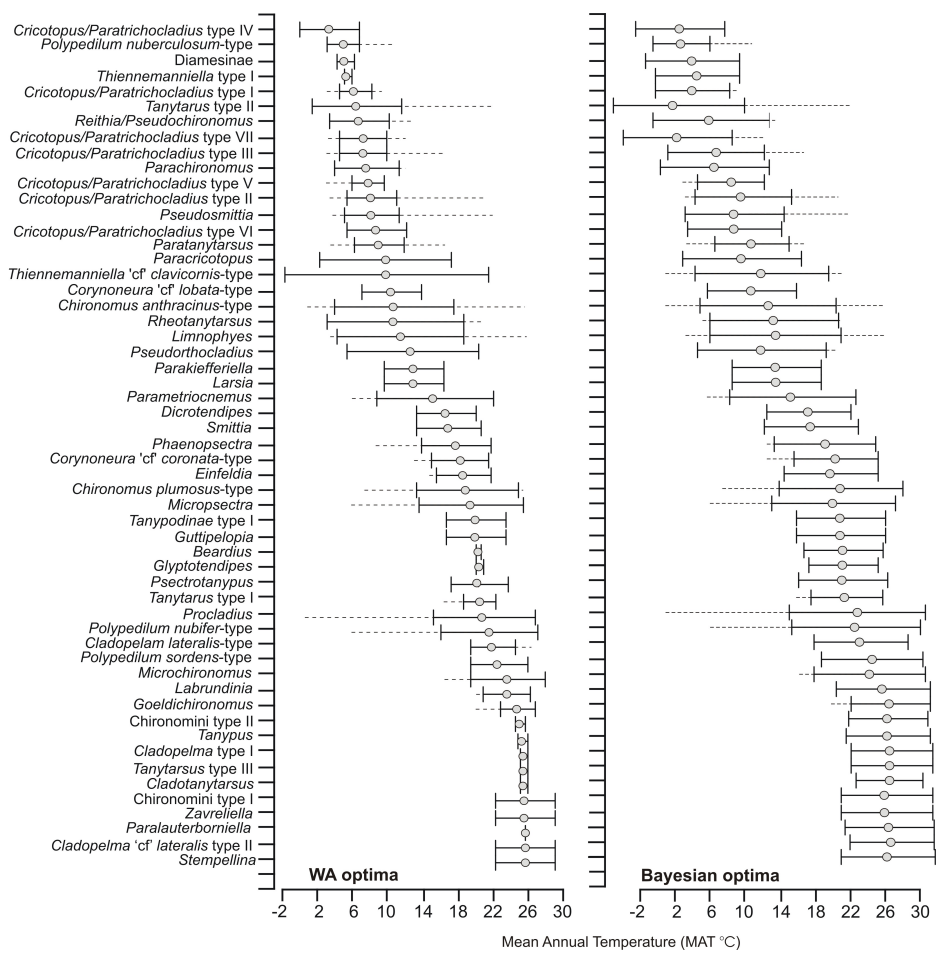
frazer 2/26/2016 2:15 PM
Deleted: <sp>

Unknown
Formatted: Font:Bold

209
210
211
212
213
214
215
216
217
218
219
220
221
222
223
224
225
226
227
228
229
230
231
232
233
234

Figure 5

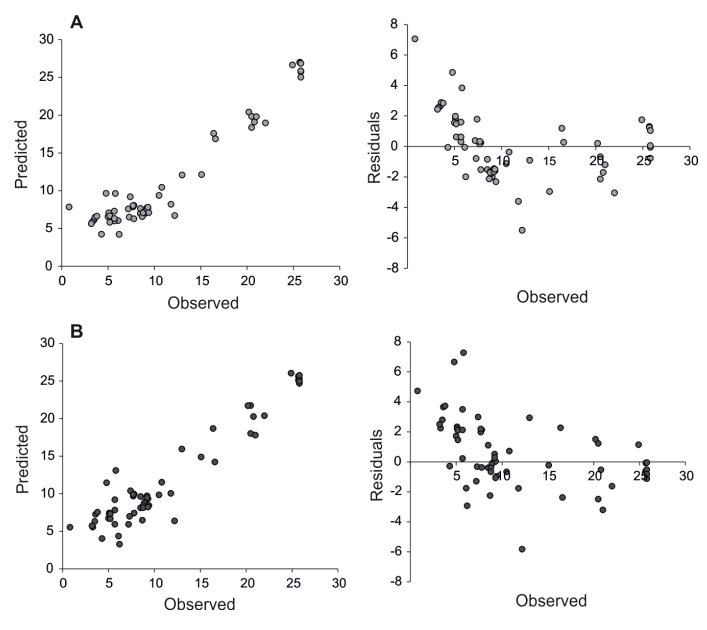
frazer 2/26/2016 3:44 PM
Deleted: 4



236
237
238
239
240
241
242
243
244
245
246
247
248
249
250
251
252
253
254
255
256
257
258
259
260
261

Figure 6

frazer 2/26/2016 3:44 PM
Deleted: 5



263

264 **Figure 7**

265

266

267

268

269

270

271

272

273

274

275

276

277

278

279

280

281

282

283

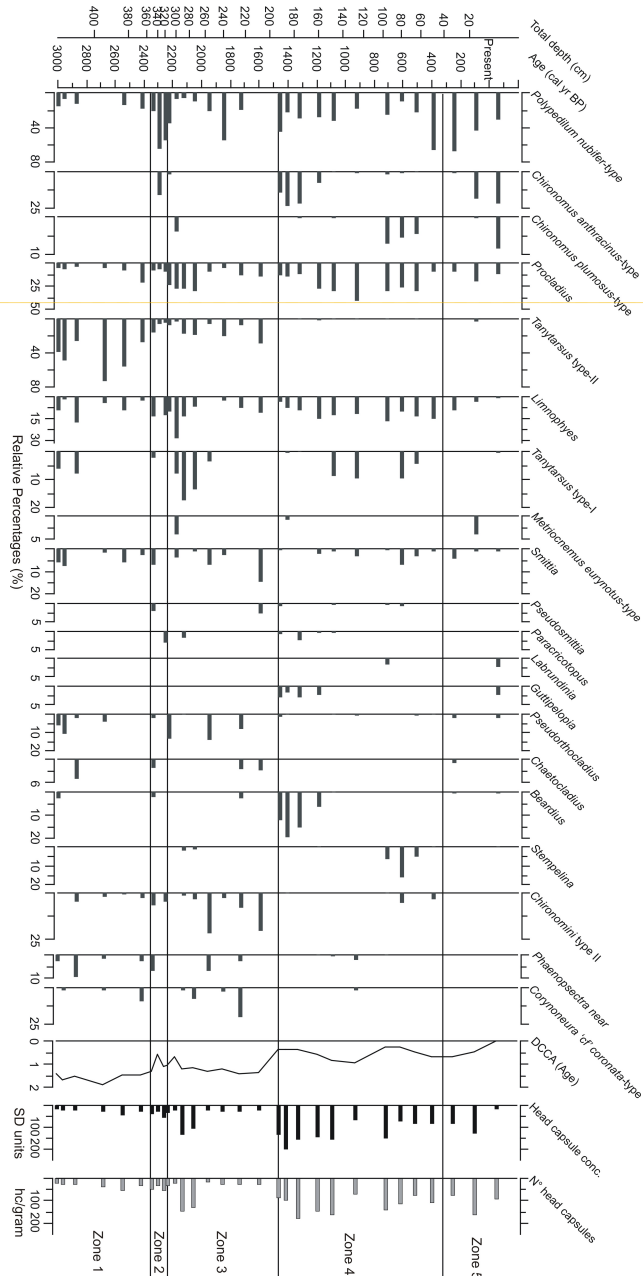
284

285

286

287

288



frazer 2/26/2016 3:44 PM
Deleted: 6

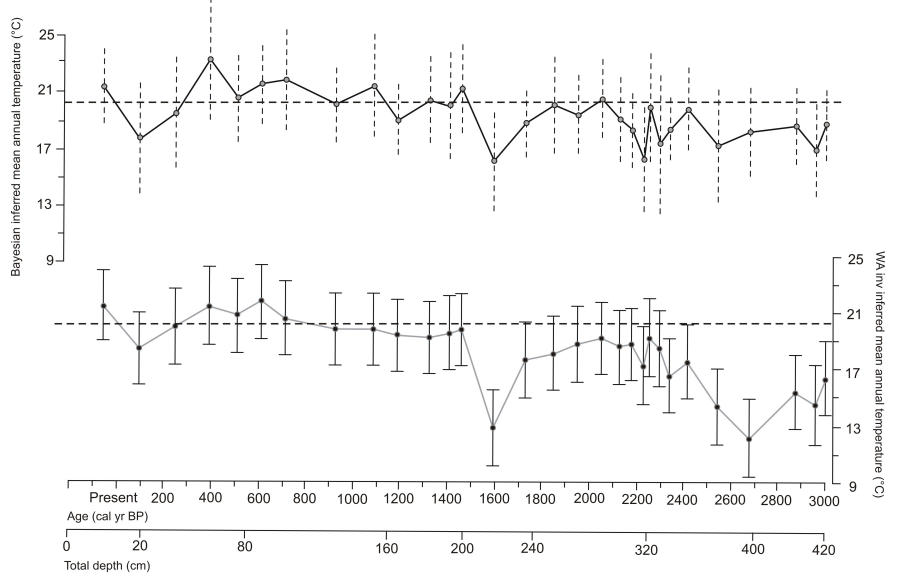
Unknown
Formatted: Font:Bold

290
291
292
293
294
295
296
297
298
299
300
301
302
303
304
305
306
307
308
309
310
311
312
313
314
315

Figure 8

frazer 2/26/2016 3:44 PM
Deleted: 7

Unknown
Formatted: Font:Bold



317

318 **Figure 9**

319

320

321

322

323

324

325

326

327

328

329

330

331

332

333

334

335

336

337

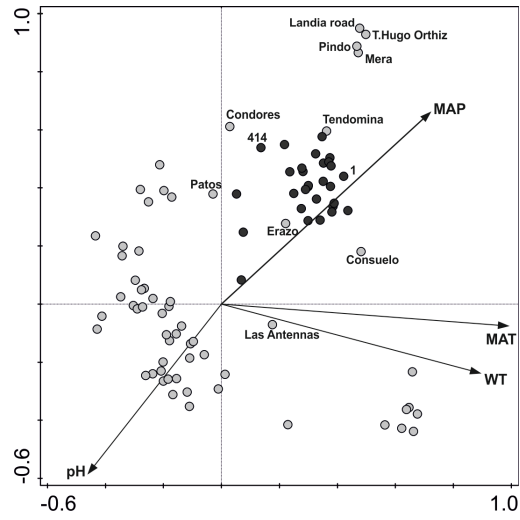
338

339

340

341

342

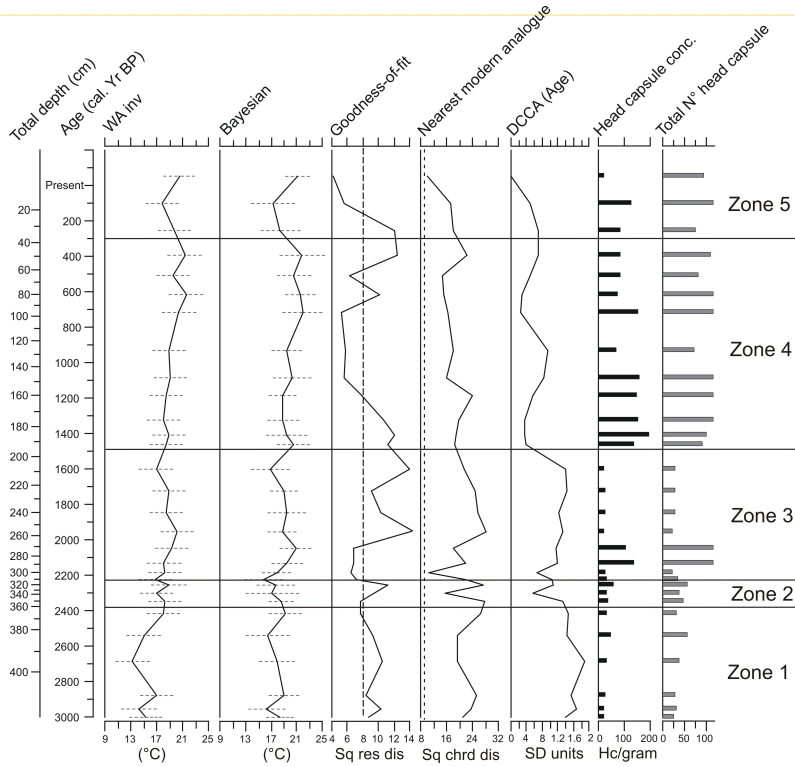


frazer 2/26/2016 3:44 PM Deleted: 8

frazer 2/25/2016 2:42 PM Deleted: ... [12]

346
347
348
349
350
351
352
353
354
355
356
357
358
359
360
361
362
363
364
365
366
367
368
369
370
371

Figure 10

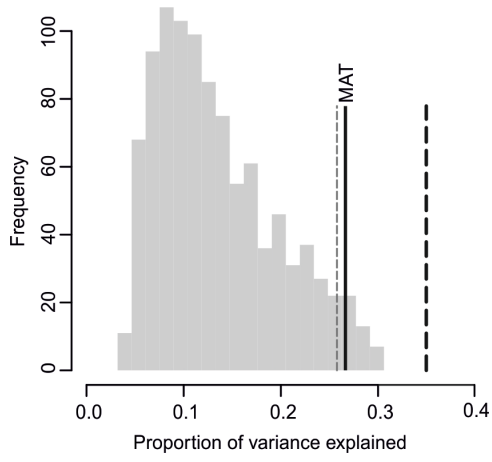


frazer 2/26/2016 2:17 PM
Deleted: <sp>
Unknown
Formatted: Font:Bold
frazer 2/26/2016 3:44 PM
Deleted: 9
Unknown
Formatted: Font:Bold

374
375
376
377
378
379
380
381
382
383
384
385
386
387
388
389
390
391
392
393
394
395
396
397
398
399

Figure 11

frazer 2/26/2016 3:44 PM
Deleted: 0



401
402
403
404
405
406
407
408
409
410
411
412
413
414
415
416
417
418
419
420
421
422
423
424

Figure 12

frazer 2/26/2016 3:45 PM
Deleted: 1

